발 간 등 록 번 호
11-1360000-001359-10
ISSN 2093-9590

Volume 8
MAY, 2019

Asia-Pacific GAW on Greenhouse Gases

Newsletter

National Institute of Meteorological Sciences
책임운영기관

Korea Meteorological Administration

KRISS

MET Malaysia

BMKG

ipen

IITM

Volume 8 MAY, 2019

Asia-Pacific GAW on Greenhouse Gases

Newsletter

Published by NIMS in May, 2019

Asia-Pacific GAW on Greenhouse Gases

Newsletter

Volume 8
MAY, 2019

National Institute of Meteorological Sciences
책임운영기관

Korea Meteorological Administration

KRISS

MET Malaysia

BMKG

ipen

IITM

contents

Global Atmosphere Watch Activities in Korea

Yuwon Kim*, Haeyoung Lee, Jae-cheon Choi, Hoanseung Kim, Seongwoon Noh, Jae-il Lee, Jungja Park, Sanghoon Kim

Korea Meteorological Administration

The Korea Meteorological Administration (KMA) began its activities related to the Global Atmosphere Watch (GAW) Programme of World Meteorological Organization (WMO) at Sobaek Mountain in 1987. It has focused on measuring atmospheric chemical composition and its long-term variations, to provide reliable scientific data and information on the chemical composition of the atmosphere and its natural and anthropogenic change, and to help improve the understanding of climate change. In addition, the KMA has expanded its contribution to the GAW Programme activities in various fields — e.g., running the GAW central facilities and training and education course, participating in pilot projects and intercomparison campaigns, and acting as a member of scientific advisory groups. Meanwhile, the Administration has recently concentrated on combining observations under the GAW Programme with other observations from the atmosphere and oceans in order to provide useful information to the public.

Monitoring Activities

The KMA has four main stations for the atmosphere watch, which are located in the west (at Anmyeondo, Chungnam Province), south (at Gosan, Jeju), and east (at Pohang and Ulleung, Gyungbook Province) of the Korean Peninsula, respectively, with an aim of monitoring the transportation of atmospheric substances and variation in the atmospheric composition over the Korean Peninsula. In collaboration with institutes in Korea, the stations collect observational data from seven auxiliary stations run by universities or research institutes in Korea. Among them, six stations were designated as GAW regional stations: Seoul

(GAW ID: SEO), Gosan (GAW ID: GSN), Pohang (GAW ID: POH), Jeju Gosan (GAW ID: JGS), and Anmyeondo (GAW ID: AMY) in the Korean Peninsula, and King Sejong (GAW ID: KSG) in the Antarctic. In addition, the KMA has a new plan to add more stations in the center and urban areas of the Peninsula to reinforce the observation network.

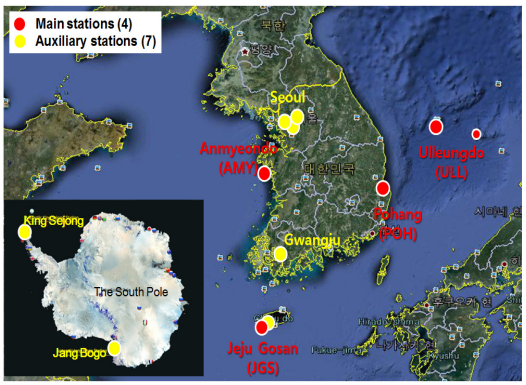

Figure 1

Location of the atmospheric watch stations operated by KMA. Four main stations (red) located in the west, south, and east of the Korean Peninsula are operated by KMA. Seven auxiliary stations (yellow) designated by KMA are run by Seoul National University (SNU), Yonsei University (YU) and SookMyung Women's University (SMWU) at Seoul, Gwangju Institute of Science and Technology (GIST) at Gwangju, Jeju University (JU) at Gosan, and the Korea Polar Research Institute (KOPRI) in the Antarctic.

The KMA monitors 36 components in the fields of greenhouse gases, reactive gases, aerosols, UV, stratospheric ozone, atmospheric radiation, and total atmospheric deposition, in accordance with the measurement recommendations of GAW Programme (see Table 1). Based on the monitoring results, every July, it publishes a Korea Global Atmosphere Watch Report in Korean and its summary in English, which show the results of observations along with QA/QC methods, causes of data missing, and specific notes. According to the 2017 Korea Global Atmosphere Watch Report, the annual mean CO_2 in 2017 was the highest at Anmyeondo (412.2 ppm), followed by Gosan (411.8 ppm) and Ulleungdo (409.7ppm). The global mean CO_2 mole fraction in 2017 from the WMO was 405.5 ppm, which is 6.7 ppm lower than that of Anmyeondo station. The annual mean of other greenhouse gases — CH_4, N_2O and SF_6 — have increased by 5 ppb, 1.4 ppb, and 0.1 ppt, respectively, in 2017 as compared to 2016, whereas the CFCs have decreased because of the Montreal Protocol, marking the lowest annual mean since observations began in 1999. For more detailed information, you can download this Report on the website (http://www.climate.go.kr/home/bbs/list.php?code=25&bname=report).

Table 1. Atmospheric species related to the WMO GAW Programme, collected at four main stations (Anmyeon, Gosan, Ulleung and Pohang) and seven auxiliary stations managed by KMA and KMA-designated institutes in the Korean Peninsula.

Site (Institute)	Greenhouse Gases	Reactive Gases	Aerosols	Stratospheric Ozone/UV	Atmospheric radiation	Total atmospheric deposition
Anmyeon (KMA)	CO_2,CH_4,N_2O, CFCs,SF_6	CO, O_3,SO_2,NOx	Physical[1] Optical[2] Chemical[3]	TCO[4],UV-A, UV-B	Solar Terrestrial	Acidity Conductivity Ions[5]
Gosan (KMA)	CO_2,CH_4,N_2O, SF_6	CO, O_3,SO_2,NOx	Physical[6] AOD	TCO, UV-A, UV-B	Solar Terrestrial	Acidity Conductivity Ions
Ulleung (KMA)	CO_2,CH_4	CO	Physical[7] AOD	UV-A, UV-B	Solar Terrestrial	Acidity Conductivity Ions
Pohang (KMA)				TCO, Profile[8], UV-A, UV-B		
Gosan (JU)		Radon				
Gwangneung near Seoul (SNU)	CO_2fluxinforest					
Seoul (YSU)				TCO, UV-A, UV-B		
Seoul (SMWU)	H_2O[9] in Stratosphere			TCO		
Gwangju (GIST)			Optical[10]			

1) PM10 mass concentration and aerosol size distribution (0.01-20 ㎛)
2) Aerosol scattering & absorption coefficients, aerosol optical depth (AOD), vertical profiles of aerosol backscattering coefficient, depolarization ratio, and color ratios
3) Water soluble ions (F-,Cl-,NO3-,SO42-,Na+,NH4+,K+,Mg2+,Ca2+)andinorganicelements(Al,Ca,Fe,K,Mg,Na,S,Ti,Mn,Zn,Cu,V,Cr,Co,Ba,Pb,Nietc.)
4) Total column ozone
5) F-,Cl-,NO3-,SO42-,Na+,NH4+,K+,Mg2+,Ca2+
6) PM10 mass concentration, aerosol size distribution (0.5-20 ㎛), total particle number concentration (0.01-3 ㎛)
7) PM10 mass concentration, aerosol size distribution (0.5-20 ㎛)
8) Vertical profile of ozone concentration measured by ozone-sonde
9) Vertical profile of water vapor measured by microwave radiometer
10) AOD, vertical profiles of aerosol backscattering coefficient, depolarization ratio, and color ratios

Cooperation on the GAW Activities in Korea

The KMA is going to integrate Korean domestic GAW-related activities and share its observational data with universities and research institutes. The first step is to integrate the GAW activities conducted at Gosan, Jeju, and to construct the Korea aerosol LIDAR observation network.

1. Collaboration with universities and institutes in GAW activity at Gosan, Jeju

The Gosan area in Jeju Island has many institutes conducting atmospheric composition measurements, e.g., KMA, Seoul National University (SNU), Kyungpook National University (KNU), Yonsei University (YU), Korea University (KU), Jeju National Universities (JNU), and Korea Environment Corporation (KECO). The KMA makes a comprehensive set of measurements

under the umbrella of the GAW Programme, as well as producing data of greenhouse gases, reactive gases, aerosols, stratospheric ozone and ultraviolet radiation, atmospheric radiation, and atmospheric chemistry. In particular, the greenhouse gas measurement system operated by the KNU is part of the Advanced Global Atmospheric Gases Experiment (AGAGE) network.

To integrate these multiple observations by several institutes and share their output, the KMA formed a consultative group, renovated the infrastructure of the site, and installed new inlets for greenhouse gases and aerosols in accordance with the GAW recommendations in 2016. These efforts allowed the KMA to have a strong scientific supporting program with appropriate data analysis and interpretation, in cooperation with research institutes and universities under the consultative group. To enhance the effectiveness and application of the long-term measurements within GAW, we also cooperate with the atmospheric measurement networks worldwide along with focusing on the quality assurance and control. The integrated station is well-suited to become a global GAW Programme given its long-term measurements of a large number of parameters and its location. We hope the station to serve as a global station for the GAW network in the near future.

2. Korea Aerosol LIDAR Observation Network (KALION)

In 2015, we constructed KALION to cope with aerosol-related atmospheric environmental issues, e.g., Asian dust, smog, haze, volcanic ashes, and fire plumes, originating from both the Asian Continent and the Korean Peninsula. Since an aerosol LIDAR (Light Detection and Ranging) instrument retrieves vertical profiles of information on aerosols, it has advantages in monitoring LIDAR measurement sites to monitor the movement of aerosols over the Korean Peninsula. The instrument is run by eight institutes in Korea — Korea Meteorological Administration (KMA), National Institute of Environmental Research (NIER), Seoul Research Institute of Public Health and Environment (SRIPHE), Seoul National University (SNU), Mokwon University (MU), Hanbat University (HU), Gwangju Institute of Science and Technology (GIST), and Ulsan National Institute of Science and Technology (UNIST). In KALION, continuous observations are carried out at six sites and event observations at the other five sites. An intensive observation campaign is also conducted once a year. The KALION members run elastic-backscatter or inelastic-backscatter (Raman) LIDAR instruments with at least two wavelengths.

They basically share range-corrected raw data and vertical information on aerosols in real time using a unified signal processing algorithm via i)

aerosol optical properties, e.g., backscattering coefficients, depolarization ratios, and color ratios, ii) aerosol classification, e.g. Asian dust, pollutants, and clouds, and iii) aerosol mass concentrations. These data are shared through the KALOIN website at www.kalion.kr.

3. Domestic SAG members meeting

WMO/GAW has designated Scientific Advisory Groups and Expert Teams (ET) in each field to keep informed of scientific and technical developments and advise its members of the developments, priority areas, and progress in each field by taking into consideration user requirements. The GAW SAG and ET members are selected based on their scientific expertise, capacity, and teamwork abilities. Korea has five SAG members in the field of greenhouse gas, reactive gas, aerosol, and GURME (the GAW Urban Research Meteorology and Environment project). The KMA has established a close relationship with them, improving domestic monitoring technology and observation environments. The members also share with the KMA updated information related to current issues and GAW policies they obtained from their regular SAG meetings.

World Calibration Centre for SF_6

WMO/GAW Programme encouraged the World Calibration Centre (WCC) to help improve data quality and homogenize data from different stations and networks. The KMA has played a role as the WCC for SF_6 (WCC-SF_6) since 2012 under the MoU with the WMO. The main functions of WCC-SF_6 are a) to assist WMO members in operating GAW station to link their SF_6 observations to the WMO reference scale through comparisons with standards calibrated against CCL; b) to assist Science Advisory Group (SAG) on Greenhouse Gases in the development of the quality control procedures required to support the quality assurance of SF_6 measurement, and to ensure the traceability to WMO scale; c) to maintain standards of laboratory and SF_6 gas transfer that are traceable to WMO scale; d) to perform regular calibrations and inter-comparison campaign involving all GAW stations and labs; e) to assist in provision of training and long-term technical help for the stations; and f) to make public its involvement in the WMO GAW Programme. In this regard, we developed a standard operating procedure and calibration methods for atmospheric SF_6 measurements (WMO/GAW report No. 222 and No. 239). Also, WCC-SF_6 has organized and implemented inter-comparison experiments with CCL (Central

Calibration Laboratory, NOAA/ESRL) biennially since 2013 and with 12 labs in Europe and Asia-Pacific region from 2016 to 2017. We expanded this inter-comparison experiment at GAW stations through the audits. To date we have conducted the audits at three Global GAW stations from 2016 to 2018.

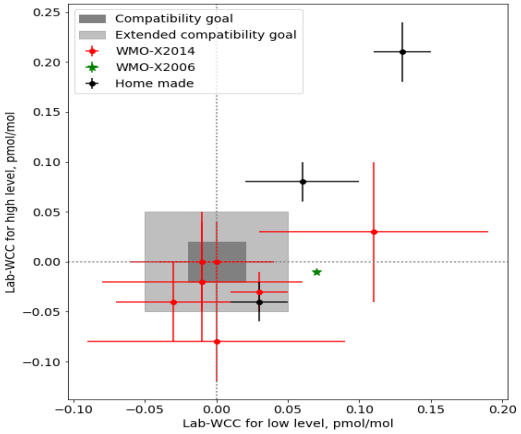

Figure 2

The Youden plot of differences between participated laboratories and WCC-SF_6. Red dots indicate WMO-X2014 scale, green dot WMO-X2006 scale, and black dots Laboratory's own scale. X-axis means the differences for low levels cylinders and y-axis for high level. CCL and WCC-SF_6 are excluded here.

The GAW community has set high data quality objectives (DQOs) that should be met by all participating stations. In this sense, WCC-SF_6 provides a training/education course with the Asia-Pacific GAW workshop on Greenhouse gases which mainly targets SF_6 monitoring stations or potential monitoring stations. In total, 25 people from 13 organizations have participated in the course from 2014 to 2018. We hope to host a regional training and education centre for atmospheric SF_6 measurements at the KMA.

Public Service on Integrated Climate Change Information Using GAW Data

The World Meteorological Organization is going ahead with the establishment of integrated information system on factors resulting in climate change while setting up a new Global Atmosphere Watch (GAW) Implementation Plan (2016-2023). Domestically, Korea has a need for more comprehensive climate change monitoring of both the Korean Peninsula and the globe for better understanding of climate change at the national level.

To shift gears from global atmosphere watch to an integrated climate change monitoring system, the KMA established an Integrated Climate Change Monitoring Information Service Plan (2017-2021) for monitoring the causes, results, and impacts of climate change, and developed a roadmap for service and its implementation based on the trends of climate change monitoring at home and abroad as well as the status of related service in different countries. Since December 2017 the KMA's climate information portal has provided information of fifteen variables – carbon dioxide, methane, nitrous oxide, sulfur hexafluoride, chlorofluorocarbons,

aerosol, ultraviolet, stratospheric ozone, surface radiation, temperature, precipitation, wind (direction, speed), sea level, sea surface temperature, and sea ice. The portal site also offers climatological significance and long-term impacts of each variable on the Korean Peninsula and related data analysis. Furthermore, the website gives users guidance on how to take advantage of the information to improve users' understanding and access to the provided contents. The portal site address: http://www.climate.go.kr/home/09_monitoring/index.php/main

(a)

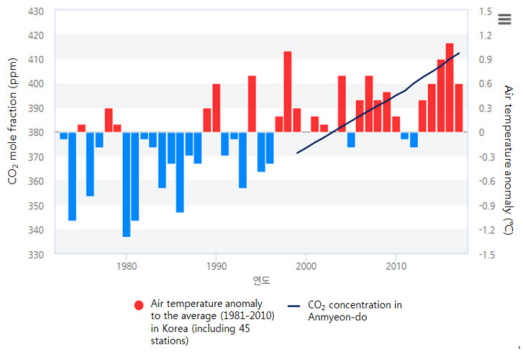

(b)

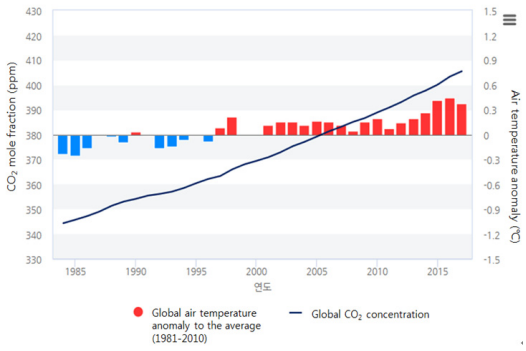

(c)

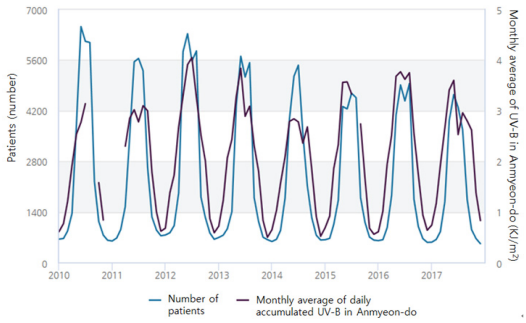

(d)

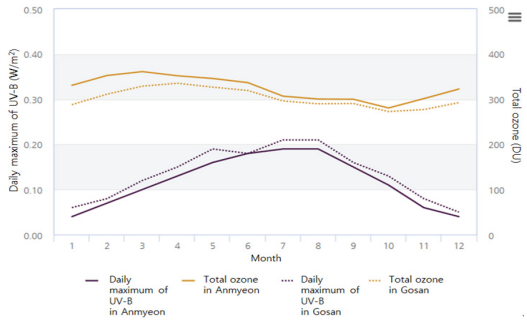

Figure 3

Examples of central graphs provided in the portal of (a) Air temperature anomaly (average: 1981-2010) and CO_2 mole fraction in Korea (b) Air temperature anomaly (average: 1981-2010) and CO_2 mole fraction in Globe (c) UV-B radiation in Anmyeondo and number of patients by skin troubles and (d) UV-B radiation and total ozone amount in Anmyeondo and Jeju Gosan

KMA's Pilot Project on WMO IG³IS

As international agreements on GHG emission are legally binding, it is necessary to provide objective and quantitative information on absorption and emission of greenhouse gases. To guide greenhouse gas emission-reduction

actions on the basis of sound scientific evidence, the WMO has implemented the Integrated Global Greenhouse Gas Information System (IG^3IS) as a global coordination mechanism. In June 2018, the WMO Executive Council (EC-70) has given its backing to the science implementation plan for IG^3IS. The KMA officially proposed a pilot project of the IG^3IS to diagnose and identify greenhouse gas emissions over East Asia and Korea, and kicked off its own project.

In the first phase (2018-2020), we are focusing on estimating reliable carbon fluxes over East Asia. To reduce the uncertainty and get multifaceted understanding about the carbon cycle, we intend to use both of the 'top-down' approach based on inverse modeling and observation data and the 'bottom-up' approach based on the climate models and inventory data.

In this regard, a study team will construct database for surface carbon flux modeling based on observation, and improve the quality of carbon simulation performance by revising land-cover and ecosystem process parameterization. Another study team will develop observation data assimilation to diagnosis carbon fluxes in East Asia, and be piloting the IG^3IS. Based on the 'top-down' and 'bottom-up' modeling systems, the research project will give an integrative understanding about uncertainties of surface carbon fluxes in East Asia as well as the base for IG^3IS with scientific and political insights.

In the first year (2018), we developed a roadmap to implement the KMA's pilot project in cooperation with scientists and researchers at the national level. Database for surface carbon flux modeling has been constructed based on observations using the bottom-up approach. Boundary data for land-surface modeling has been computed by using multiple satellite and surface measurements. To understand carbon emissions from urban areas based on the top-down approach, we evaluated the CO_2 level using remotely sensed data over the Seoul Capital Area, which is one of the apparent megacities in the world yet lacks in a network of surface CO_2 observation. We have analyzed column-integrated CO_2 (XCO_2) from the Orbiting Carbon Observatory-2 ($OCO\text{-}_2$) for the years 2015 to 2018. The annual mean of XCO_2 over the Seoul Capital Area has increased from 398.6 ppm in 2015 to 409.2 ppm in 2018. This increasing trend, about 2.4 ppm yr^{-1} over the four years, is consistent with the CO_2 trends observed in

surface stations (Anmyeon and TaeAhn). Seasonal fluctuations of the XCO_2 can also be seen to peak in late winter and drop in late summer as shown in the surface observations. This indicates that XCO_2 can be a tool for understanding the behavior of CO_2 in an annual-mean or seasonal time scale.

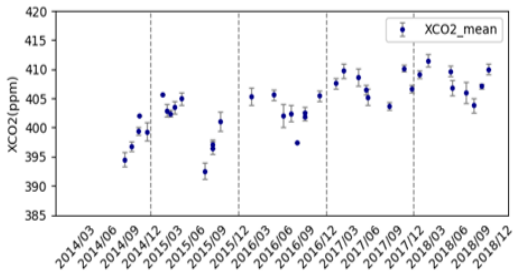

Figure 4

Time series of XCO_2 over Seoul from 2014 to 2018. Gray whiskers indicate spatial standard deviations of XCO_2 over Seoul for each observation.

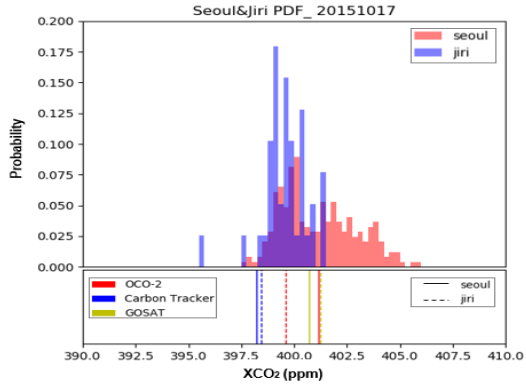

Figure 5

Probability density functions of OCO-2 XCO_2 over Seoul (Red) and Mt. Jiri region (Blue) of 17 Oct 2015. Mean XCO_2 values over Seoul (solid) and Mt. Jiri region (dashed) are indicated by vertical lines based on the OCO-2 (red), CarbonTracker (blue), and GOSAT (yellow) data in the lower panel.

We defined the urban XCO_2 enhancement as the difference of the XCO_2 between Seoul and the Mt. Jiri region, a densely vegetated area in Korea, to evaluate the local XCO_2 increase from anthropogenic activities over the Seoul Capital Area. The urban enhancement ranged from 1.4 to 2.9 ppm depending on meteorological conditions. This enhancement clearly shows the influence of urban carbon emissions on atmospheric CO_2 abundance However, for the case of the XCO_2 retrieved from the GOSAT and CarbonTracker, the urban enhancement was not captured due to relatively low spatial resolution compared to the XCO_2 retrieved from the OCO-$_2$. This implies that high resolution data is essential for monitoring urban CO_2 and assessing massive carbon emissions over megacities across the world..

Renewal of World Data Centre for Greenhouse Gases (WDCGG) Website

Mikio Ueno*

Japan Meteorological Agency (JMA), Tokyo, Japan

*Retired from JMA in March 2019. Contact

Introduction

The World Data Centre for Greenhouse Gases (WDCGG) is one of the World Data Centres (WDCs) operated by the Japan Meteorological Agency (JMA) under the Global Atmosphere Watch (GAW) Programme of the World Meteorological Organization (WMO). WDCGG was established in October 1990 and has served to collect, archive and provide data on greenhouse gases (CO_2, CH_4, N_2O, CFCs, etc.) and other related gases(CO, etc.) in the atmosphere. The WDCGG website is used to provide and update greenhouse gas observation data contributed by organizations and individual researchers worldwide (hereinafter referred to simply as contributors). Thanks to the generous support of these contributors, WDCGG has built an extensive archive of data along with GAW network development.

On 1 January 2016, responsibility for archiving of reactive gas observation data (other than for CO) was officially transferred to the newly established World Data Centre for Reactive Gases (WDCRG) hosted by the Norwegian Institute for Air Research (NILU). Reactive gas data submitted to WDCGG before 1 January 2016 are being migrated to WDCRG (Figure 1). WDCGG now archives and provides greenhouse and other related gases totaled more than 50 species (Figure 2).

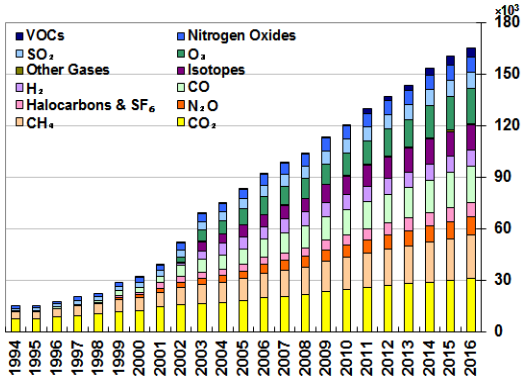

Figure 1

Data amount archived at WDCGG. O_3, SO_2, Nitrogen Oxides and VOCs data are being migrated to WDCRG.

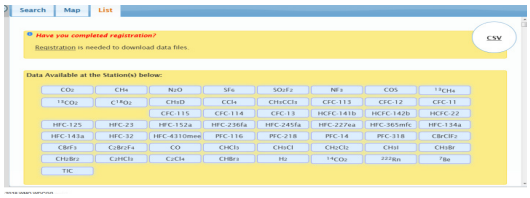

Figure 2

Gas species available at WDCGG website.

Launch of the new website

The new WDCGG website was launched on 31 August 2018 and the Figure 3 shows its homepage (https://gaw.kishou.go.jp/). The former website (http://ds.data.jma.go.jp/gmd/wdcgg/) was closed on 30 November 2018. WDCGG had reviewed requests for the former website from both users and contributors and made the following major changes on its website to incorporate some of them;

(a) Change of data submission procedures

(b) Introduction of user registration

(c) Change of data file format

These changes have benefited for both users and contributors.

These changes have benefited for both users and contributors.

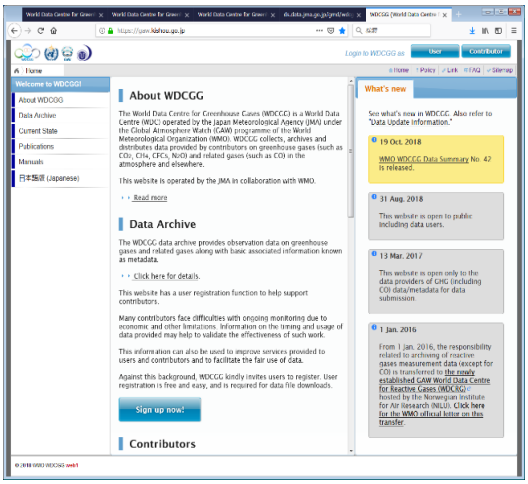

Figure 3

Homepage of the new WDCGG website.

(a) Change of data submission procedures

Contributors used to submit data files to WDCGG by email or by ftp. Since they were supposed to update metadata on the website, it sometimes happened that the contributors failed to update metadata even if needed. To avoid this, contributors can now upload data files on the new website immediately after checking/updating the associated metadata by following three steps of the data submission procedures (Figure 4). This change has strengthened links between measurement data and the associated metadata so that users can have properly updated metadata.

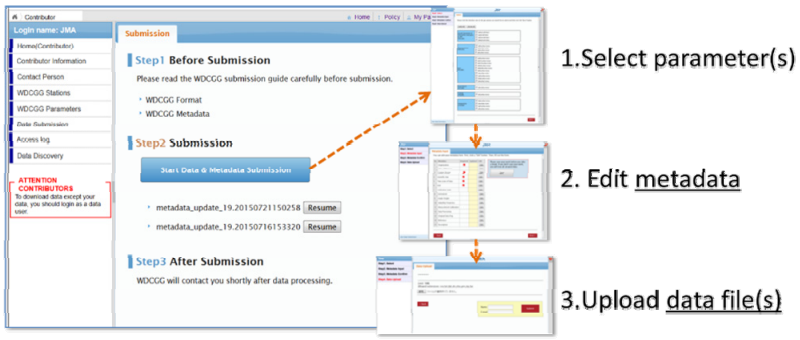

Figure 4

Data submission procedures on the new WDCGG website.

(b) Introduction of user registration

Quite a few contributors requested WDCGG to give information on data downloading. The main reason was that they were experiencing cases where some users did not post an acknowledgment within a publication despite downloading and using data from WDCGG, which is against the GAW data policy[1]. In response to the request, user registration has been introduced to the new website so that contributors can obtain information on users who downloaded their data.

As with the former website, users can browse data plots or search for the metadata on the new website without user registration (Figure 5).

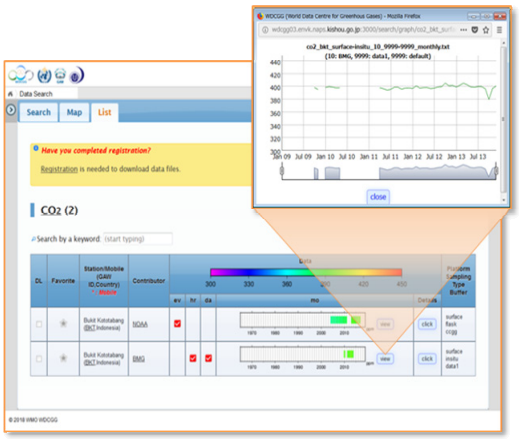

Figure 5

Example of data plots on the new WDCGG website.

(c) Change of data file format

The data file format has been modified to provide more detailed metadata and to facilitate data processing. In the old format, the number of lines of the header part including metadata was fixed to 32. The new format has flexibility in number of lines, making it much easier to add metadata. The format of the data part, it differed for each observing platform. In the new format, the same format is used in the data part in the new format regardless of platform.

Future plans

WDCGG has plans to improve some functions of the website. One is to archive and provide data observed by satellites such as Greenhouse gases Observing SaATellite (GOSAT), Orbiting Carbon Observatory-2 (OCO-2). As the first step, CO_2 data from GOSAT will be archived early in 2019. Another is to provide data files in netCDF format.

Summary

The new WDCGG website was launched on 31 August 2018. Three major changes on the website, change of data submission procedures, introduction of user registration and change of data file format, have been made to provide benefits for both users and contributors.

WDCGG now archives and provides greenhouse and some other gases totaled more than 50 species on its website. In the near future, it will start providing satellite data on its website. WDCGG also has a plan to provide data files in netCDF format.

Acknowledgments

WDCGG thank all of the contributors for their submission of greenhouse gas measurement data and metadata to WDCGG.

Reference

[1] WMO (2002): Commission for Atmospheric Sciences (CAS) - Thirteenth session: abridged final report with resolutions and recommendations, WMO No.941.

Activities of WCC for Methane in Asia and the South-West Pacific

Teruo Kawasaki[1]*, Masamichi Nakamura[1], Kazuyuki Saito[1], Kentaro Kozumi[1], Genta Umezawa[1], Kazuya Yukita[1], Shigeharu Nishida[1], Megumi Yamamoto[1], Yousuke Sawa[2], Kazuhiro Tsuboi[2], Kentaro Ishijima[2] and Hidekazu Matsueda[2]

1. Japan Meteorological Agency (JMA), Tokyo, Japan
2. Meteorological Research Institute (MRI), Tsukuba, Japan

Introduction

The Japan Meteorological Agency (JMA) serves as the World Calibration Centre (WCC) for methane (CH_4) and the Quality Assurance/ Science Activity Centre (QA/SAC) in Asia and the South-West Pacific within the framework of the Global Atmosphere Watch (GAW) Programme of the World Meteorological Organization (WMO). As part of the WMO/ GAW quality assurance system, the WCC-JMA has a fundamental role to help to ensure the traceability of GAW network measurements to the WMO primary standard through comparison campaigns and performance audits at GAW sites.

Primary standards

The WCC-JMA has two sets of CH_4 primary standards that were assigned on the WMO CH_4 mole fraction scale at NOAA. Both sets of primary standard gases were volumetrically prepared in 48-L aluminum high-pressure cylinders by JMA in cooperation with a Japanese gas company Japan Fine Products (JFP). The CH_4 mole fractions in the primary standard gases range from approximately 1610 to 2160 nmol mol^{-1}, thus covering the natural variability of CH_4 in well-mixed background air. The stability of the CH_4 contents in all of the primary gas cylinders has been carefully monitored since 2011.[1][2]

Calibration system for WCC-JMA

From the establishment of the WCC-JMA in 2001 until only recently, its methane calibration system was based on a gas chromatograph equipped with a flame ionization detector (GC/FID). However, over the past few years laser-based spectroscopic techniques such as wavelength-scanned cavity ring-down spectroscopy (WS-CRDS) have become commercially available for the measurement of atmospheric CH_4. These techniques provide higher precision, improved stability, lower maintenance, and easier operation than the GC/FID method. Thus, the WCC-JMA replaced the existing GC/FID system with a new calibration system using WS-CRDS analyzer in 2017.[3]

Using the two sets of CH_4 primary standard gases, we tested the performance of the new calibration system. Figure 1 shows the frequency distribution of standard deviations (SDs) for five repetitive measurements of CH_4 with the new WS-CRDS system for several reference gas samples calibrated during March–October 2017. 88% of the SDs were less than 0.1 nmol mol^{-1}; SDs larger than 0.16 nmol mol^{-1} were obtained for only 3 of the 199 calibrations done. We evaluated the measurement repeatability of the new calibration system to be 0.06 nmol mol^{-1} (median of the SDs). Thus, the introduction of the WS-CRDS calibration system at JMA improved the repeatability of CH_4 standard gas calibrations by one order of magnitude, compared with the previous GC/FID with the repetitive analytical precision of ~1.2 nmol mol^{-1}.[3][4] We also examined the CH_4 mole fractions calibrated by both the GC/FID and WS-CRDS systems in order to assess the consistency in the continuity of calibration. The CH_4 mole fractions for all 15 reference gases covered the range from 1600 to 2200 nmol mol^{-1}. The GC/FID mole fraction used to determine the difference between the WS-CRDS and GC/FID mole fractions obtained for each reference gas was calculated by using the average value for all calibrations by the GC/FID method. The differences between the results of the two calibration methods for the 15 reference gases ranged from −0.35 to +0.57 nmol mol^{-1} (Fig. 2) and showed no dependency on CH_4 mole fraction. These results indicate the consistency of standard gas calibrations by both methods with a combined analytical uncertainty of ±0.4 to ±1.3 nmol mol^{-1} (Fig. 2). The average of the differences for all the reference gas measurements was +0.21 ± 0.27 nmol mol^{-1} (n = 15), indicating a small statistically insignificant positive bias. These results suggest that instrument bias of the WS-CRDS analyzer caused by the isotope effect and the pressure-broadening effect were minimal.

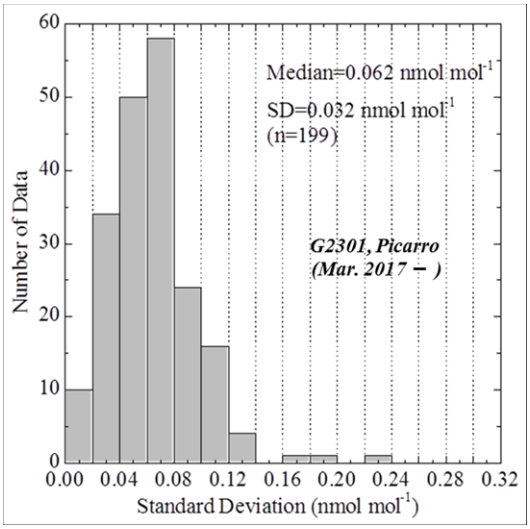

Figure 1

Frequency distribution of standard deviations for five repetitive measurements of CH_4 mole fractions in one calibration run using the new WS-CRDS calibration system during March–October 2017.

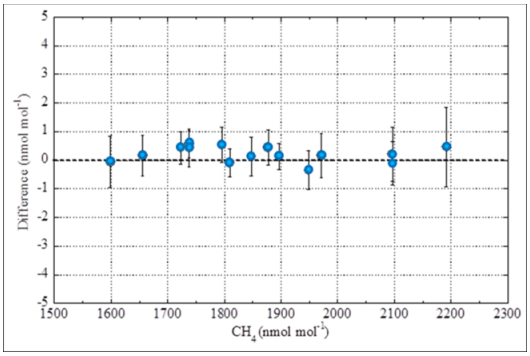

Figure 2

Differences between CH_4 mole fractions measured by the WS-CRDS and GC/FID calibration systems for 15 reference cylinders with mole fractions covering the range 1600–2200 nmol mol^{-1}. Error bars show combined measurement uncertainty calculated from the standard deviations of both calibration measurements.

Reference gas inter-comparison

The WCC-JMA organized four rounds of the CH_4 reference gas inter-comparison experiments from 2001 to 2016 as part of the WCC activities in Asia and the South-West Pacific in cooperation with NOAA (WMO/CCL, USA), CSIRO (Australia), NIWA (NewZealand), CMA (China), KMA/KRISS (Republic of Korea), IITM (India), MRI (Japan), NIES (Japan), AIST (Japan), NIPR (Japan), and TU (Japan); the fifth and sixth rounds are still in progress. The purpose of the inter-comparisons is to understand the differences between the participant's CH_4 standard scales as well as to monitor the long-term stability of standard gases in Asia and the South-West Pacific. Figure 3 shows a conceptual diagram of the CH_4 reference gas inter-comparison experiments. In these experiments, two cylinders of reference gas with different CH_4 mole fractions are circulated in turn to participating laboratories for measurement of their mole fractions; the measured values are reported to the WMO/GAW Secretariat through the WCC-JMA. Details of the inter-comparison experiments and their results are available from the WCC-JMA website (https://ds.data.jma.go.jp/wcc/wcc.html). So far, there are no participating institutions from the region surrounded by a red line (Fig.3). We expect that all observation institutions in this region will participate in the inter-comparison

experiments in the future.

The inter-comparisons allow evaluation of the long-term performance of calibrations by JMA and other participating laboratories and their consistent traceability to the WMO mole fraction scale by comparison of direct measurements of reference gas samples from the same cylinders. Figure 4 shows the temporal variations of the differences between the WCC-JMA and the other laboratories. All of the WCC-JMA measurements are calculated based on the WMO mole fraction scale. The measurement results by each institution are converted to the WMO mole fraction scale using conversion coefficients.[5][6] However, institutions that do not have conversion coefficients to the WMO mole fraction scale are not plotted in this figure. In recent years, all of the laboratories show a good agreement within the GAW compatibility goal of ±2 ppb.[7]

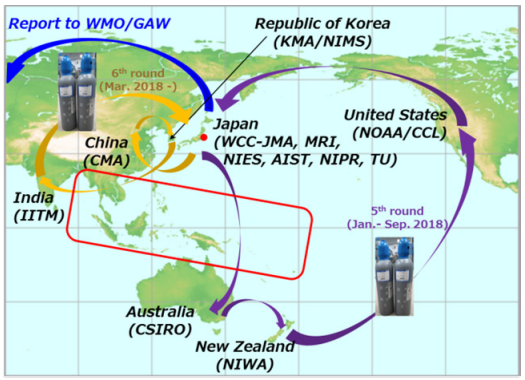

Figure 3

Conceptual diagram of the CH_4 reference gas inter-comparison (round-robin) experiments.

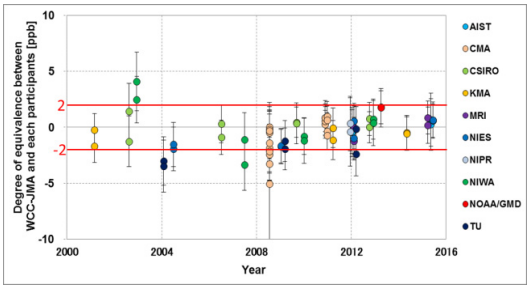

Figure 4

Temporal variations of the differences between WCC-JMA and each participant, as revised on WMO mole fraction scale. Error bars show combined measurement uncertainty calculated from the standard deviations of each measurement.

Other inter-comparison activities in Japan

The JMA and major Japanese laboratories (AIST, NIPR, NIES, TU, MRI, and NMIJ), forming a national alliance to standardize observation data on greenhouse gases, conducted Inter-Comparison Experiments for Greenhouse Gases Observation (iceGGO). The purpose of the iceGGO is to examine the differences between the GHG standard gas scales used for atmospheric observations as well as to evaluate the consistency of the scales with the International System of Units traceable standard gases prepared by the gravimetric method of the National Metrology Institute of Japan. The program performed six round-robin experiments for carbon dioxide (CO_2), methane (CH_4), carbon monoxide (CO), and nitrous oxide (N_2O) during the period 2012–2016. An additional experiment was also carried out using round-robin

cylinders provided by NOAA. Throughout the seven experiments, the iceGGO program was successful in precisely determining the differences between the standard gas scales. For details of experimental methods and results for all experiments, see reference[6].

Acknowledgments

We thank all of the participating laboratories for their contribution to the WCC inter-comparison experiments.

Reference

[1] Tsuboi et al. (2016): Scale and stability of methane standard gas in JMA and comparison with MRI standard gas, Pap. Meteorol. Geophys., 66, 15-24, doi:10.2467/mripapers. 66.15.

[2] Hosokawa et al. (2016): Asia-Pacific GAW on Greenhouse Gases Newsletter vol.7 8-12.

[3] Matsueda et al. (2018): Evaluation of a new methane calibration system at JMA for WCC Round Robin experiments, Pap. Meteorol. Geophys. 67, 57-67, doi:10.2467/mripapers. 67.57.

[4] Matsueda et al. (2004): Methane standard gases for atmospheric measurements at the MRI and JMA and intercomparison experiments. Pap. Meteorol. Geophys., 54, 91-109, doi:10.2467/mripapers.54.91.

[5] Dlugokencky et al. (2005): Conversion of NOAA atmospheric dry air CH_4 mole fractions to a gravimetrically prepared standard scale, J.Geophys. Res., 110, D18306, doi:10.1029/2005JD006035.

[6] Tsuboi et al. (2017): InterComparison Experiments for Greenhouse Gases Observation (iceGGO) in 2012–2016, Technical Reports of the Meteorological Research Institute, No.79, 1-72, doi:10.11483/mritechrepo.79.

[7] World Meteorological Organization (WMO), (2018): 19th WMO/IAEA Meeting on Carbon Dioxide, Other Greenhouse Gases and Related Measurement Techniques (GGMT-2017), GAW Report, No.242, 1-4.

Seasonal Analysis of Atmospheric Greenhouse Gas at the Danum Valley Global Atmospheric Watch Station

Mohan Kumar Sammathuria*, MaznorizanMohamad

Malaysian Meteorological Department, Petaling Jaya, Malaysia

Introduction

Global Atmospheric Watch (GAW) monitoring activities had been carried out at the Danum Valley GAW Station for nearly 2 decades. The different monitoring activities undertaken at this GAW site includes measurements of greenhouse gases, aerosols, reactive gases and precipitation chemistry.

Monitoring of greenhouse gases at the Danum Valley GAW Station is very crucial as the Borneo Island in not only one of the biggest carbon sinks in the world[1] but also being very close to the equator, this region is synonymous with the rising motion of the Hadley Cycle, which allows for global transport of atmospheric composition composition.

The Danum Valley GAW station is located in the north east of the Borneo Island with geographical coordinates of 04°58'53"N and 117°50'37"E. The elevation of the station is 426 m above sea level and it is located in a Class 1 Protected Forest Reserve, therefore it can be minimized the potential for anthropogenic activity occurring in the vicinity. Such conditions are necessary to allow regional representation of the background atmospheric composition measurements undertaken.

Measurement approach

Greenhouse gas measurements at the Danum Valley GAW station are undertaken using an analyzer and the flask sampling collection system. A LoFlo Mark II CO_2 Analyzer had

been in operation since 2006 to 2016. The LoFlo measures carbon dioxide mole fraction based upon a differential nondispersive infrared (NDIR) optical bench. Presently a Picarro G2401 and a Licor-840 are being lent to the Malaysian Meteorological Department (MMD) by the National Institute of Environmental Studies (NIES), Japan to enable continuity of the greenhouse gas measurements while awaiting the MMD to procure its own greenhouse gas analyzer. The flask sampling collection system in place is also lent to the MMD by NIES and has been operational since November 2010. The greenhouse gas analyzer data employed for this research exercise will be limited to the data collected using the LoFlo analyzer and flask sampling from 2011 to 2016.

Data obtained during the first ten minutes in an hour for the LoFlo continuous analyzer correspond to one reference cylinder. After the reference gas injection, six minutes allows for flow rate and pressure stabilization. therefore enabling observation data at one minute resolution are 44 minutes data during each hour of observation. The hourly averages computed are based upon these 44 minute data and similarly the daily average is then computed using the hourly averages. The LoFlo is calibrated every 4 to 6 weeks using 7 calibration cylinders.

The flask sampling approach is used to measure carbon dioxide, methane, nitrous oxide, sulphur hexafluoride and carbon and oxygen isotopic ratios. The flask air sample is collected between 10 pm to 10.10 pm every Sunday. This sampling time was selected due to atmosphere at the Danum Valley GAW Station being relatively stabilized between 10 pm to 12 am local time, The affects due to absorption/release of CO_2 due to photosynthesis and respiration respectively are minimal during this two hour interval[2]. (Nomura et al, 2018).

Result and anlysis

Although the LoFlo analyzer had been in operation since 2004, nevertheless regular continuity of data was only established as of June 2011. from June 2011 to December 2016, the data was generally continuous with the exception of a three month period from Mar 2015 to May 2015 (Figure 1). Most data were well within the standard deviation range of 3 ppm or around 0.8%. General pattern of carbon dioxide observed by LoFlo analyzer at the Danum Valley GAW Station from June 2011 to December 2016 conforms its increase similar to global trend and Mauna Loa from 2006 to 2013. (Figure 1),[3] increase recorded at Mauna Loa from 2006 to 2013.

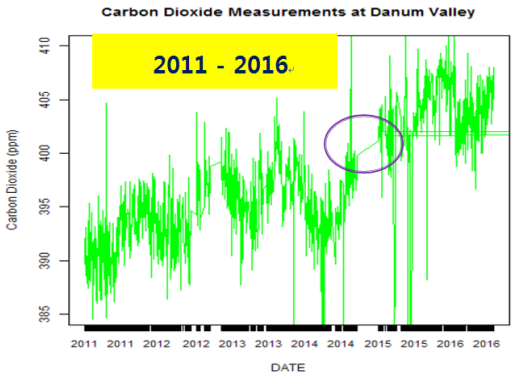

Figure 1

Daily average CO_2 at the Danum Valley GAW Station from 2011-2016

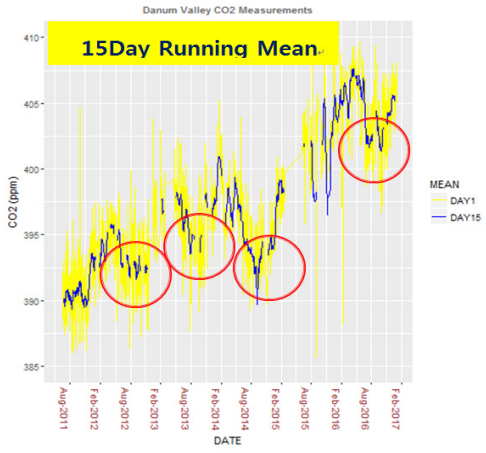

Figure 2

15-Day Running Mean for daily average CO_2 at the Danum Valley GAW Station from 2011-2016

A 15-day running mean was calculated to pick out any significant cycle within the background of the increasing global atmospheric carbon dioxide. A significant drop in carbon dioxide could be established clearly during the months of Jun, July, August and September on an annual basis. These significant drops are demarcated by the red circles in Figure 2. This drop was not indicated for 2015 in Figure 2 given the unavailability of LoFlo analyzer data from Mar. 2015 to May 2015 and September of 2015. The significance for the relative dip of CO_2 mole fraction from June to September results in the clear seasonal cycle in Figure 3.

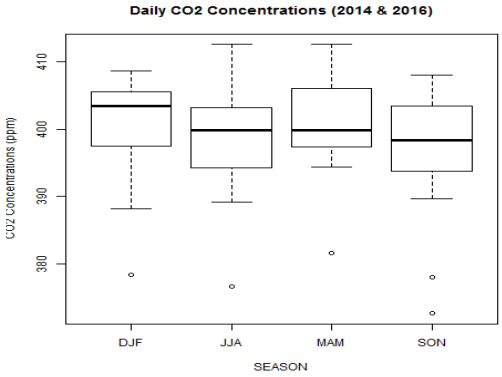

Figure 3

Distribution of seasonal CO_2 level computed by daily mean at the Danum Valley GAW station in 2014 and in 2016.

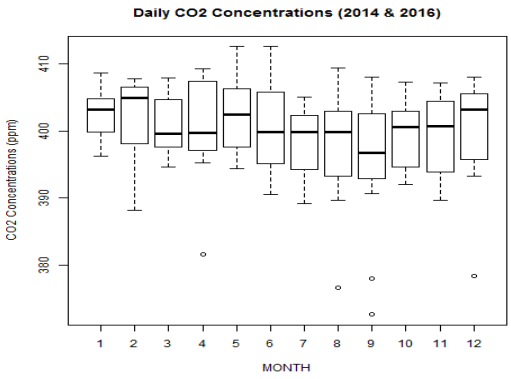

Figure 4

Distribution of monthly CO_2 level computed by daily mean at the Danum Valley GAW station in 2014 and in 2016.

The seasonal (Figure 3) and monthly analysis (Figure 4) were conducted only in 2014 and 2016 given that during these two years the data was complete throughout the year. Meanwhile in 2012, 2013 and 2015 there were one, two and four months without data respectively. Measurements undertaken during the six month period, December-January-February (DJF) and March-April-May (MAM) demonstrate evidently higher carbon dioxide compared to the remaining six months, Jun-July-August (JJA) and September-October-November (SON). Carbon dioxide mole fraction was significantly highest during DJF compared to the rest of the seasons The CO_2 level in JJA and SON were generally similar. Looking at the Seasonal variation in 2014 and 2016 (Figure 4), the monthly level of carbon dioxide starts decreasing from May onwards until the minimum is reached in September, and then begins to increase again until the highest distributions are recorded in December, January and February.

Figure 5

General Synoptic wind directions in the South China Sea during December-January-February (DJF) (Yellow Arrows) and Jun-July-August (JJA) (Red Arrows).

General wind patterns in southern Southeast Asia during the Boreal winter and summer monsoons are displayed in Figure 5. During the boreal winter monsoon, the winds over this region are northerly to easterly over the region. During the boreal summer monsoon the winds are predominantly southerly to westerly over the region. During the inter-monsoon period of between Mar and May and September and October the winds are generally light and variable. The seasonal cycle of CO_2 derived from 15-day running mean is in sync with weakening or absence of a notherly to easterly regional winds across the northern Borneo. The carbon dioxide measurements undertaken by the LoFlo analyzer being the highest during the months of December, January and February clearly demonstrate the significance of the northerly to easterly wind component in transport of the carbon dioxide to norther Borneo. The lowest values recorded during July, August and September (Figure 4) coincide with the period during which the southerly to westerly wind component is strong and the northerly to easterly penetration in to the region at its weakest.

Therefore carbon dioxide clearly indicate significantly for temperate countries to be the source of net transport of carbon dioxide to Borneo The relative proximity of temperate countries in East Asia and developing countries in Southeast Asia such as Viet Nam and the

Philippines provides strong justification to assume that the net carbon transported to Borneo can originate from those region. Performing backward trajectories employing air quality models for an adequate period should be able to determine the most prominent trans-boundary source of CO_2 to Borneo, among the different regions above. These findings also demonstrate the importance of equatorial forest cover such as in Borneo and across other forested regions of southern Southeast Asia as global sinks for greenhouse gases in general.

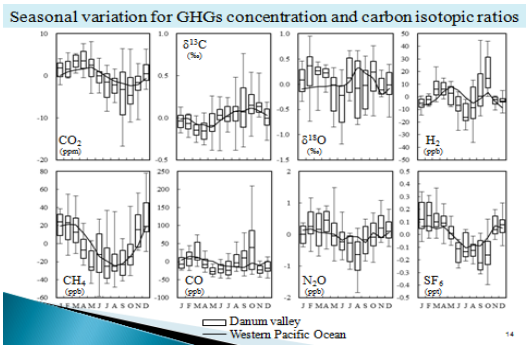

Figure 6

Distribution of greenhouse gases and carbon isotropic ratios measured using flask sampling at the Danum Valley GAW Station from 2011 – 2016. - **Adapted from [4].**

Monthly analysis of the measurements for various greenhouse gases and carbon isotopic undertaken from 2012 to 2017 using the flask sampling approach at the Danum Valley GAW Station site is displayed in Figure 6 above. Consistent with the analysis based upon carbon dioxide measurements undertaken at the Danum Valley GAW Station using the LoFlo Mark II analyzer, a similar pattern of greenhouse gases namely carbon dioxide, methane, sulphur hexafluoride and nitrous oxide, reducing and increasing during the Boreal winter and summer monsoon respectively is obtained. This consistency in analysis for all the greenhouse gases mentioned above demonstrates the relevance of investigating northerly to easterly winds related net transport of all these pollutants from north to near equatorial regions such as the Borneo Islands.

The concentration of $\delta^{13}C$ varies corresponding to carbon fixation in plants due to photosynthesis, during which 12C is released to the atmosphere via the production of photosynthesis based methane.

Therefore an increase in methane due to photosynthesis usually results in reduction of $\delta^{13}C$. Concentrations of $\delta^{13}C$ and CH_4 decreasing and increasing respectively from around October up to Mar (Figure 6) demonstrate the significant role of northerly winds as agents of transport for agriculture based methane. An important source for nitrous oxide is coal fired power plants. Sulfur hexafluoride is the most potent greenhouse gas and is entirely anthropogenic.

Conclusion

Net transport of greenhouse gases to the Borneo Islands consistent with the strength of the northerly to easterly wind component suggest

that greenhouse gases observed at Northern Borneo are predominantly trans-boundary and most probably from the North. Nevertheless the most probable source region needs to be investigated employing backward trajectory modelling. The findings obtained also strengthen and reinvigorate the role of equatorial forests located in Borneo and probably in southern Southeast Asia as global sinks.

Acknowledgments

The Malaysian Meteorological Department very much appreciates the effort that NIES, Japan has undertaken to help with the Greenhouse gas measurements being undertaken at the Danum Valley GAW Station. The author would also like to personally thank the Korea Meteorological Administration for sponsor of the air fare, accommodation and meals during the entire workshop.

Reference

[1] Saatchi, S. S. et al. (2011): Benchmark map of forest carbon stocks in tropical regions across three continents, Proceedings of the National Academy of Sciences, 108(24), 9899-9904, 2011.

[2] Nomura et al, (2018). Evaluation of forest CO_2 fluxes from sonde measurements in three different climatological areas including Borneo, Malaysia and Iriomote and Hokkaido, Japan, Tellus B: Chemical and Physical Meteorology, 70:1, 1426316.

[3] Jahaya, M. F. et al. (2013): The Greenhouse Gases Observations and Analysis at GAW stations in Malaysia, Asia-Pacific GAW Greenhouse Gases Newsletter, Vol. 4, December 2013, ISSN 2093-9590.

[4] Nomura et al. (2018): 3rd International Forum On Sustainable Future in Asia, 3rd NIES International Forum, January 23 – 24, 2018, Kuala Lumpur, Malaysia.

Greenhouse Gases Monitoring Activities in Bukit Kototabang

Tanti Tritama Okaem*

The Indonesia Agency of Meteorology, Climatology and Geophysics (BMKG), Indonesia

Station Overview

Bukit Kototabang GAW Station is located in west Sumatra of Indonesia. The location which is characterized by tropical rain forest with minimum human activities is in the 17 km North of Bukittinggi and 120 km North of Padang, the capital city of west Sumatra Province. The station is in equatorial zone (0.20 S and 100.32 E), 864,5 meters above sea level. The station can be reached by car with small street access for about 3 km from avenue Padang and Medan. Bukit Kototabang GAW station conducts observation of Green House Gases (GHGs), Reactive Gases, Wet Deposition, Aerosol Mass and Basic Meteorology.

Figure 1
General views of Bukit Kototabang GAW Global Station

Method

Greenhouse gases (GHGs) monitoring activity in the station has been commenced since 2004 with air flask sampling method. The air sample

conducted on weekly time base is collected in a pair of 2.5 L flasks. Flask samples are shipped to NOAA ESRL for further analysis. The flasks containing ambient air taken from a 32 meter height inlet. In 2008, a Picarro G1301 $CO_2/CH_4/H_2O$ analyzer was installed at the station. The instrument provides a continuous measurement, allowing the observers to get near-real time data. A year later, an automated inlet and calibration system were added to support the measurement of the existing Picarro. The system, which was installed by MeteoSwiss and WCC-Empa, enables the instrument to automatically measure the GHG mole fraction of ambient air from three height levels, as well as to perform calibration up to three different level[1]. Unfortunately in early 2015, Picarro has been stopped working due to instability of the electricity at the station.

In 2018, GHGs are monitored by using Picarro G2401 Cavity Ring-Down Spectrometer (CRDS). The sample of G2401 with 16-Port Distribution Manifold sequentially was drawn up to 16 gas sources[2]. The instrument can be used on isotopic and/or concentration analyzers that measure CO_2, CO, CH_4 and H_2O. The system is same with Picarro G1301 that automatically measure the GHGs of ambient air from three height levels (10 m, 20 and 30 m).

Results

Over the last 10 years, the GHG mole fraction measured at Bukit Kototabang have been used for representing the profile of GHGs in a remote tropical rainforest area in Indonesia[1]. All measured GHGs have been increasing started from the first data.

The trends from 2004-2017 focused on CO_2, SF_6, N_2O and CH_4 data using Air Kit Flash Sampler, because the new instrument (Picarro G2401) needs calibration before using. Figure 2 is tranding CO_2 in Bukit Kototabang GAW station.

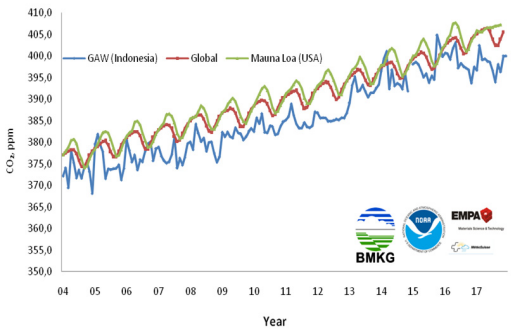

Figure 2

Observed CO_2 in Bukit Kototabang GAW station compared with global and Mauna Loa

The concentration of CO_2 in the atmosphere varies over time, with significant ups and downs experienced by the planet over geological times. A steep rise in carbon dioxide clearly is started at the industrial revolution[3]. In Figure

2, it can be seen that CO_2 mole fraction is continuously increasing since the beginning of measurement. CO_2 annual mean in Bukit Kototabang has been increasing from 373.1 ppm in 2004 to 398.5 ppm in 2017. CO_2 in Bukit Kototabang GAW station is still under global and Mauna Loa while Average annual growth rate of CO_2 for this period is 2.3 ppm/year.

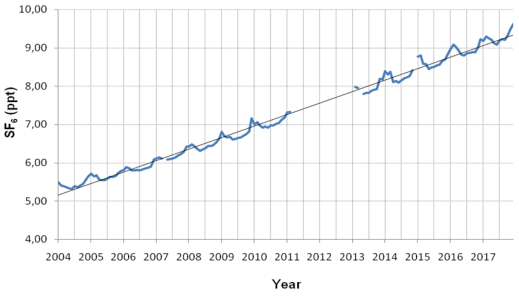

Figure 3

Observed SF_6 in Bukit Kototabang GAW station

Sulfur Hexafluoride (SF_6) is greenhouse gas with atmospheric lifetimes of more than 1000 years. Even though the amount in the atmosphere is completely small compared to the main greenhouse gases like carbon dioxide, the huge lifespan of this gas in atmosphere makes it important in global greenhouse gas. It can be seen from Figure 3 that SF_6 level increased from 5.43 ppt in 2004 to 9.27 ppt in 2017. It increased 3.84 ppt or almost 70% higher than its initial value.

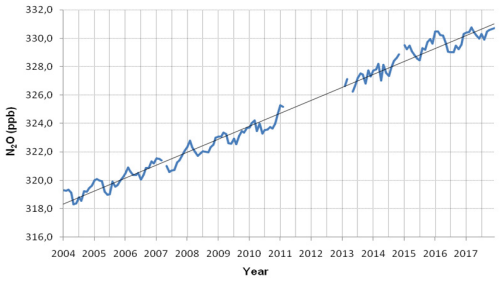

Figure 4

Observed N_2O in Bukit Kototabang GAW station

Nitrous Oxide (N_2O) measured at Bukit Kototabang is continuously increasing similar to CO_2 and SF_6 concentrations. This trend is presented in figure 4 above. N_2O mole fraction increased from 319.1 ppb in 2004 to 330.4 ppb in 2017. Average annual growth rate of N_2O is 0.87 ppb/year.

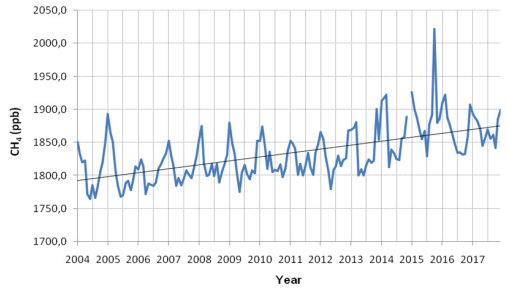

Figure 5

Observed CH_4 in Bukit Kototabang GAW station

Methane (CH_4) is a greenhouse gas that is much stronger than carbon dioxide (CO_2). It is 34 times stronger if compared over a 100-year period. While amount of methane in the atmosphere are about 200 times lower than carbon dioxide. Methane was responsible for 60% of the

equivalent radiative forcing caused by carbon dioxide since the onset of the industrial revolution[4]. In October 2015, Indonesia was experienced severe fire forest that increased CH_4 mole fraction. CH_4 level increased from 1811 ppb in 2004 to 1870.8 ppb in 2017 and the highest value is 2021.3 ppb in 2015.

System and Performance Audit

In January 2019, team from Empa-Switzerland came to Bukit Kototabang to perform system and performance audit of several measurement parameters. Those parameters are CO_2, CH_4, CO, surface ozone, SO_2 and N_2O.

The audit for CO_2, CH_4 and CO was conducted with Picarro G2401 by inter-comparing the reading from the instrument to the known three standard gases, for calibration was using inlet with 30 meter height inlet.

Figure 6 is comparison the data from the new instrument Picarro G2401 Bukit kototabang with WCC-EMPA Switzerland.

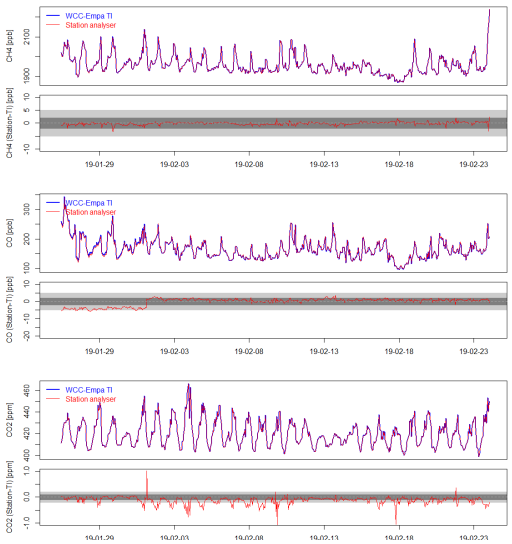

Figure 6

Comparison measurement CH_4, CO, CO_2 Bukit Kototabang with WCC-EMPA

Reference

[1] Nahas A. C. (2014): A decade of greenhouse gas monitoring activities in Bukit Kototabang, Indonesia, Asian GAW Greenhouse Gases Newsletter Vol 5, p 22-25.

[2] Henry et al. 16-Port Distribution Manifold A0311 user Guide. Santa Clara, CA 95054 USA. 40-0038 Rev.F

[3] Beaudry F. (2018): Methane Carbon Dioxide: The No. 1 Greenhouse Gas.thoughtco

[4] Dean J. (2018): Methane, Climate Change, and Our Uncertain Future, Earth & Space Science News, 99, https://doi.org/10.1029/2018EO095105

First 4 years of greenhouse gases monitoring activities at the Pha Din GAW Regional station, Viet Nam

Nguyen Nhat Anh[1]*, Hoang Anh Le[2], Martin Steinbacher[3]

1. Hydro-Meteorological Observation Center (HYMOC), Viet Nam Meteorological and Hydrological Administration (VNMHA), Ministry of Natural Resources and Environment of Viet Nam (MONRE)
2. Faculty of Environmental Sciences, VNU University of Science, Vietnam National University
3. Swiss Federal Laboratories for Materials Science and Technology (Empa), Switzerland

The Vietnamese Government has considered climate change to be one of national key missions in recent years. It was concretized through policy document of the Government and the Ministry of Natural Resources and Environment (MONRE).

On that basis, Pha Din Global Atmosphere Watch (GAW) Regional station was invested and constructed within the framework of the project CATCOS (Capacity Building and Twinning for Climate Observing Systems). Pha Din GAW station was launched to aim at strengthening the climate monitoring on global scale, particularly in developing countries and countries in transition. Monitoring data of Pha Din GAW Regional station will also contribute to strengthening the capacity of Vietnam in assessing the status of greenhouse gas (GHGs) emissions and air quality in a more comprehensive scale.

Overview and description of Pha Din GAW Regional station

Pha Din is the first GAW Regional station in Viet Nam (21.57°N 103.51°E,1466m a.s.l.) and it was installed at the Pha Din meteorological station on the North-West high mountain belonging to Toa Tinh precinct, Tuan Giao district, Dien Bien province. In early 2014, the

instrumentation of trace gases (CO_2, CO, CH_4 and O_3) and aerosols optical properties began to be installed at Pha Din station. WMO accepted Pha Din station as a GAW Regional station at the Letter No. 5549-14/RES/AER/ Viet Nam dated on 25th July 2014. Pha Din station is located in a region where GHGs measurements are sparse. The station is located on the top of a hill, lying in a rural area and is surrounded by forest. The sample inlet is on 12 m above ground, which is above the canopy, an important feature for the CO_2 measurements, which would otherwise be influenced by uptake and respiration by the nearby vegetation.

Figure 1
Location and terrain of Pha Din GAW station

In 2013, within the framework of the MOU between VNMHA (former National Hydro-Meteorological Service - NHMS) and Federal Office of Meteorology and Climatology MeteoSwiss, construction of Pha Din station was done, including the preparation for installation of measuring equipments, procurement of materials and auxiliary equipment. Atmospheric composition monitoring instruments at Pha Din station include:

- Picarro G2401 Cavity Ringdown Spectrometer (CRDS) measuring $CO/CO_2/CH_4/ H_2O$.
- Thermo TE49i UV absorption analyzer for measuring O_3.
- Aerosols analyzers: Aurora 3000 Nephelometer and Magee Scientific Aethalometer AE31.
- Calibration equipment and six gases cylinders.
- Data acquisition computers.
- Other accessories.

Figure 2
Instruments of Greenhouse gases and Aerosols

After installation of monitoring equipment and testing, Swiss experts of Paul Scherrer Institute (PSI) and Swiss Federal Laboratories for Materials Science and Technology (Empa) have trained the operating staffs at Pha Din station and transferred technology to VNMHA.

The measured data is transferred to VNMHA via FPT servers. GHGs data is processed by R software for filtering and archiving the data while aerosols data is processed by CPX2 software. Once a year, all data is prepared for submission to the World Data Centre for Greenhouse Gases (WDCGG) and the World Data Centre for Aerosols (WDCA).

Figure 3

Training and transferring technology

Major results of GHGs measurement at Pha Din station and initial assessments

After 4 years (2014-2017) of implementation of measuring GHGs, first conclusions can be drawn out of the GHGs time series of Pha Din which are showed in Figure 4.

Two ranges of very high CO_2 mole fraction were observed, which can not be explained by the station's e-log book: In June 2015, and from end of September 2015 to beginning of October 2015 with maximum value of 550 and 650 ppm CO_2, respectively. Meanwhile, maximum hourly mean of CO reached 1500 ppb in early 2014 and again present an increase in Spring (February – April) for the years 2015 to 2017. Besides, CO mole fraction show a similar picture of CO_2 except the periods of very high CO_2 from June to October 2015 mentioned above. These are illustrated in the monthly average plot in Figure 5.

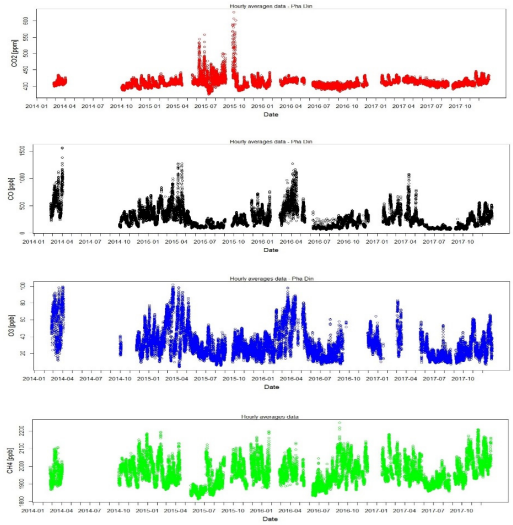

Figure 4

Hourly average time series of trace gases at Pha Din station

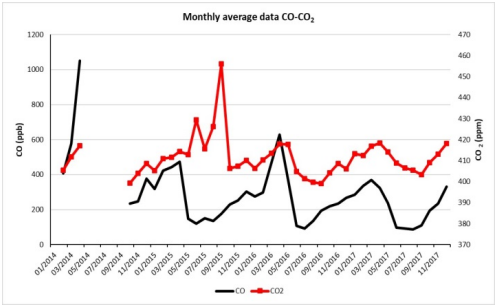

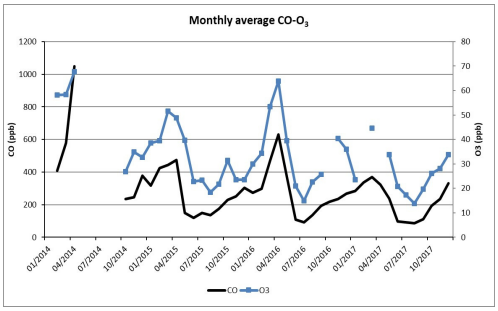

Figure 5

Correlation between CO-CO_2 (left) and CO-O_3 (right)

The maximum levels of both gases CO and CO_2 usually increase in the Spring annually, with the highest in April. During these periods, the air masses arriving at Pha Din have the majority coming from Southwestern area (Thailand, Myanmar, and Laos). The FLEXTRA backward trajectory model also illustrates this trend (see Figure 6). This evolution is perfectly in accordance with the land fire hotspot listed by ASMC because these periods are consistently characterized by no rainfall and low relative humidity (see Figure 7).

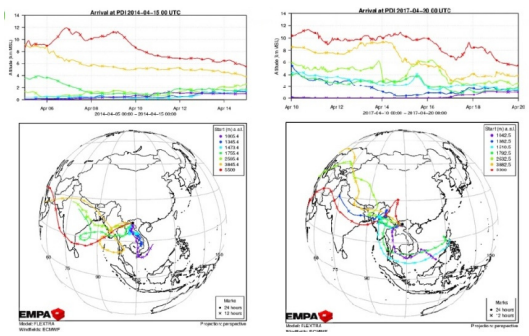

Figure 6

Backward trajectories calculation for April 2014 (left) and 2017 (right)

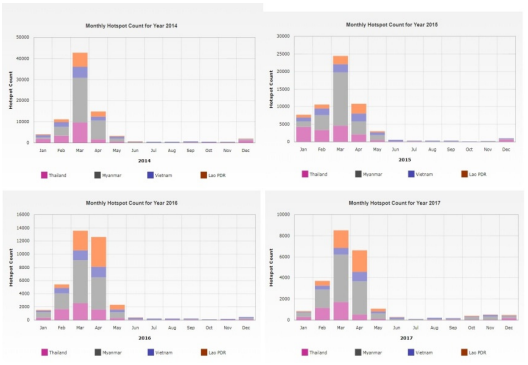

Figure 7

Land fire hotspots in Viet Nam and other surrounding countries from 2014 - 2017

Similar to the CO_2 and CO the time series of O_3 have a high variation in early every years. Furthermore, O_3 is formed locally by advection of CO and VOCs from biomass burning and due to higher NOx emissions (see Figure 5). Finally, methane (CH_4) showed a seasonal cycle with maximum mole fraction in winter time. The agricultural activity in rice paddies in entire Southeast Asia leads to important bacterial emissions during the no-growth season in winter, which is reflected in the measurements.

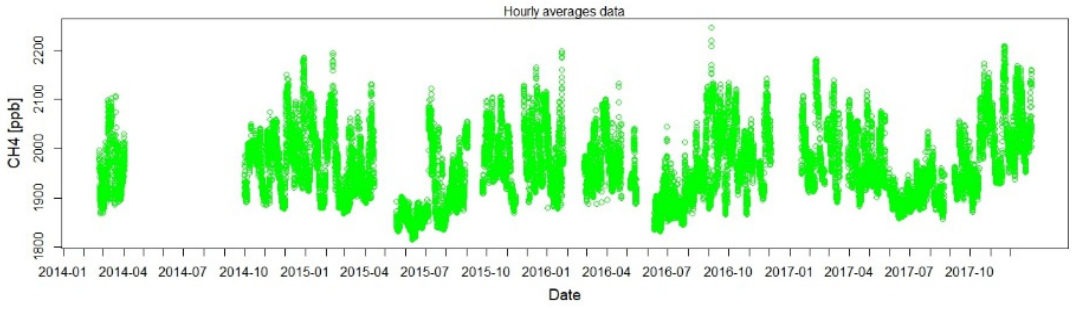

Figure 8

Time series of CH_4 for 4 years

Difficulties in operation and maintenance of instruments at Pha Din station

Pha Din is located in high mountainous areas, so the quality of transmission of the power supply and internet is not stable, sometimes the power supply is off causing interruption of measurement. During the operation of the station, sometimes the instruments have trouble or malfunction. However, it can not be fixed in time due to difficult conditions on human resources on-site. Due to hard natural conditions in Vietnam (hot-wet and rainfall climate) and continuous operation 24/24 h, the equipment at the station are susceptible to be broken suddenly. While the funds allocated for the task of checking and troubleshooting at station is quite limited. Therefore, it is very difficult to ensure stable and continuous operation. Price of GHGs observing equipment is very high, so spare parts for it are relatively expensive. This is a great difficulty for Viet Nam in the current economic context. Moreover, the experience of the management and operation team of the station is lacking so the results are still limited.

Proposal and suggestion

Strengthen the coordination between GAW stations in the Asia - Pacific region in particular and globally in general to exchange and share experiences in operation and maintenance of instruments at station. Provide additional support in capacity building for managing and operating staffs of the station by giving workshops and training courses related to GHGs monitoring programs similar to this one. VNMHA is now considering to submit to the MONRE for funding to maintain the annual operation of Pha Din GAW station. There should be an effective coordinative mechanism to assist countries that are facing difficulties in technology such us training as well as financing in order to maintain stable operation of GAW stations in these countries,

including Pha Din GAW station.

Reference

[1] The Project CATCOS (Capacity Building and Twinning for Climate Observing System).

[2] Memorandum of Understanding (MOU) between Federal Office of Meteorology and Climatology (MeteoSwiss) and National Hydro-Meteorological Service of Viet Nam (NHMS) with reference to the project CATCOS signed in May 27, 2013.

[3] Trinh et al. (2014): Greenhouse Gases Measurement in Viet Nam. Asia-Pacific GAW Greenhouse Gases Newsletter Volume No.5 December, 2014.

[4] Empa's FLEXTRA GAW trajectories browser. https://lagrange.empa.ch/FLEXTRA_browser/index.php.

[5] ASMC. http://asmc.asean.org/asmc-haze-hotspott-monthly#Hotspot.

Long-term Study of Greenhouse Gases Emissions in Brazilian Amazon Basin and Next Steps

C. S. C. Correia[1,2]*, L. V. Gatti[1,2], L. G. Domingues[1,2], R. S. Santos[1,2], S. P. Crispim[2], R.A.L. Neves[2], L. Marani[2], E. U. Gloor[3], J. B. Miller[4], W. Peters[5].

1. Nuclear and Energy Research Institute, IPEN-CNEN/SP, Brazil;
2. National Institute for Spaces Research, INPE/CCST, São José dos Campos-SP, Brazil;
3. University of Leeds, Leeds, United Kingdom;
4. National Oceanic and Atmospheric Administration, NOAA, Boulder-Colorado, United States.
5. University of Groningen, Groningen, Netherlands

Since the year of 2000 our group is working in cooperation with NOAA to better understand the Amazon Basin contribution in the global scenario of greenhouse gases (GHG) emissions. Previously the measurements were performed in NOAA laboratory in Boulder, CO, USA. In 2003 a replica of the laboratory was constructed and since 2004 the measurements are performed in Brazil, firstly the laboratory was named Atmospheric Chemistry Laboratory and it was hosted at IPEN (Nuclear and Energy Research Institute), from 2004 to 2015 and later, until the present date, by INPE (National Institute for Spaces Research) and then renamed as LaGEE (Greenhouse Gases Analisys Laboratory).

The Amazon rainforest is one of the vastest tropical forests in the world, corresponding for 50% of this biome in the globe. It has a total area of, approximately, 8 million km^2, which 5 million km^2 are in Brazil (58.74% of the total area in Brazil) and contains one quarter of global biodiversity, the greatest part of GHG emissions in Brazil are from land use change, agricultural activities and biomass burning, the forest is under constant pressure due to these factors [1],[2]. Studing and understanding its behavior and changes are critical to the whole world.

Because the studied region and the analysis laboratory are over two thousand kilometers apart, instead of moving the laboratory to a closer facility, we sample natural air in glass flasks using small aircraft over sites in

Amazon, initially in 2000 and until 2009, only in Santarém (SAN; 2.86ºS, 54.95ºW). In 2010 the program included more sites in order to have a great quadrant to better understand the whole Brazilian Amazon Basin area: Alta Floresta (ALF; 8.80ºS, 56.75ºW), Rio Branco (RBA; 9.38ºS, 67.62ºW), and Tabatinga (TAB; 5.96ºS, 70.06ºW). We still perform sampling in these sites, except the last one (TAB) that changed to Tefé (TEF; 3.39°S, 65.6°W) in 2013 due to technical problems, all the sites are displayed in Figure 1.

The vertical profiles were performed using small aircrafts in a descendant helicoidally pattern, in which a flask is sampled in a pre-determined altitude from top (4500 m) to bottom (300 m). The inlet was installed in the aircraft such the gases from its engine combustion wouldn't interfere in the sample, it was also installed a temperature and relative humidity sensor and also a GPS in order to register the conditions and positioning of each sample. The sampling system consists of two units, one containing two pumps and rechargeable batteries and another containing the glass flasks. It was chosen to sample between 12:00 and 13:00 local time because at this time of the day the troposphere is more stable, therefore providing a better repeatability of the atmospheric conditions. This methodology is well described in [3].

Taking advantage of the fact that the studied region has an atmospheric air circulation pattern where the air entering at the Amazon basin is dominated by trade-wind easterlies coming from the tropical Atlantic Ocean (AO) in direction to Andes (West) it was developed a method to calculate fluxes using mixing ratios of a given studied GHG [4],[5]. This method requires background (BKG) and we use mixing ratios found in two global stations located in the AO, one in the Northern Hemisphere in Barbados (RPB) and the other one in the Southern Hemisphere in Ascension Island (ASC). In this regard we started to make measurements of samples taken in the surface of Brazilian Coastal sites in order to have these also as BKG for Amazon Basin sites. We have added in 2013, two more sites in our program with profiles from 7.3 km to 300 m in height, at Salinópolis (SAH 0.60° S; 47.37° W) by the Atlantic coast, and at the same place than RBA, located at the western Amazon, these flights were named RBH. These profiles are interesting to compare and validate satellite measurements over Amazon and also to answer one important question about what information we are missing above 4.5 km height and what is the those gases distribution between this height and 7.3 km.

In 2016, new measurements using FTIR (Fourier-transform infrared spectroscopy), a technique used to measure total column, were initiated with a partnership of BIRA-IASB / IFRO and INPE. The instrument is installed at IFRO campus in Porto Velho, RO (8.74° S, 63.87° W) (Figure 1).

Our laboratory is also interested to expand the knowledge and understanding of other important Brazilian biomes, in 2016 we started to perform aircraft sampling in Pantanal (PAN), an area that is constantly flooded from 6 to 8 months per year. In order to understand better the carbon cycle we are now starting carbonyl sulfide (COS) and CO_2 isotopes (^{13}C, 1^7O and ^{18}O) measurements. This will also provide valuable data to the community to interpret how the forest is interacting with the atmosphere.

Figure 1

Brazilian GHG measurements Program run by LaGEE/INPE laboratory, 4 Amazon aircraft sites TAB (TEF), RBA, ALF, SAN (0.3 to 4.4km) and more 2 sites up to 7.3km RBA and SAH, 3 coast sites SAL, CAM and NAT. And also PAN in Pantanal biome region.

After sampling the equipment is brought to our laboratory and the mixing ratios of each GHG is determined. The presented results in Figure 2 are the average of all flasks of each vertical profile from 2004 to 2018 for all sites and studied gases. The data shows an enhancement for all studied gases mixing ratios. In Table 1 we present the average growth rates for each GHG in their respective sampling site time series and also the average growth rate for the whole basin, in comparison with WMO GHG bulletin for the past 10 years. Some of the presented data needs reprocessing, it's pretty clear in SF_6 data, for example, in a period of the year 2016 we had some variations in the calculation of the mixing ratios. All this need to be done so this data can be available to the community.

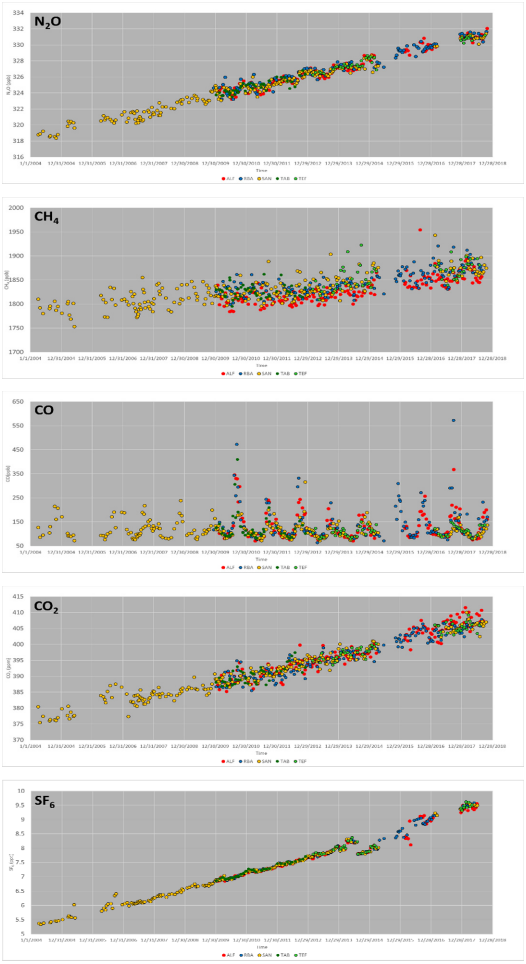

Figure 2

GHG mixing ratios average for all profiles, sites and years (2004-2018). Each color represent data found in given sampling site red for ALF, blue for RBA, yellow for SAN, dark green TAB and light green TEF.

Table 1. Growth Rate per Year for Each Site and Whole Amazon Basin Average in comparison with WMO GHG Bulletin 2018

	CO_2 (ppm yr-1)	CH_4 (ppb yr-1)	N_2O (ppb yr-1)	SF_6 (ppt yr-1)
ALF	2.71	8.38	0.96	0.36
RBA	2.54	7.71	0.97	0.36
SAN	2.16	6.37	0.91	0.30
TAB	2.15	0.74	0.77	0.25
TEF	4.01	13.70	1.55	0.65
Basin Avg	2.71	7.38	1.03	0.45
WMO	2.24	6.9	0.93	0.3

We observed that, even though our data needs more processing, the preliminary results shows that the Amazon Basin GHG mixing ratios are enhancing slightly more than the global average, in comparison to the WMO data. This means that the region needs studies in this sense to clearly understand how and what processes are interfering in GHG budgets, this way this study can contribute to the society and the world itself.

PAN has also presented some preliminary results quite interesting, though short termed until the present moment, we are focusing mainly on CH_4 data for the moment where it's possible to observe a high variation of this gas mixing ratios along a year of measurements.

The CO_2 isotopes measurements are already running, even though, more work is needed in order to better understand and interpret the results. Unfortunately the COS equipment is not yet running.

Acknowledgments

CNPq, FAPESP, NERC, MCTI, NOAA, INPE and IPEN

Reference

[1] Gloor et al. (2012): The carbon balance of South America: A review of the status, decadal trends and main determinants. Biogeosciences, 9(12), 5407–5430. http://doi.org/10.5194/bg-9-5407-2012

[2] MCTIC - Ministério da Ciência, Tecnologia, Inovação e Comunicação. Third National Communication of Brazil to the United Nations Framework Convention on Climate Change. Brasília, 2016.

[3] Gatti et al. (2014): Drought sensitivity of Amazonian carbon balance revealed by atmospheric measurements. Nature, 506(7486), 76–80. http://doi.org/10.1038/nature12957

[4] Chou et al. (2002): Net fluxes of CO 2 in Amazonia derived from aircraft observations. Most, 107(April). http://doi.org/10.1029/2001JD001295

[5] Miller et al. (2007): Airborne measurements indicate large methane emissions from the eastern Amazon basin. Geophysical Research Letters, 34(10). http://doi.org/10.1029/2006GL029213

Comparison of atmospheric nitrous oxide and carbon monoxide analyzers for high-precision measurement

Haeyoung Lee*, Sumin Kim, Miyoung Ko, Sang-Sam Lee, and Sang-Boom Ryoo

Environmental Meteorology Research Division, National Institute of Meteorological Sciences, Jeju, 63568, Republic of Korea

Introduction

Nitrous oxide (N_2O) is a powerful greenhouse gas with 0.17 [0.13 to 0.21] $W \cdot m^{-2}$. The global warming potential (GWP) of N_2O is 298 times greater than that of carbon dioxide (CO_2) over a 100-year time horizon due to its long life time[1]. CO results in atmospheric drivers for climate change due to its impact on the life time of CH_4 or the photochemical products of O_3 and CO_2 once it is emitted into the atmosphere[2]. CO has indirect forcing relating to the chemical reaction, which is estimated to be 0.23 [0.16 to 0.3] $W \cdot m^{-2}$.

Normally, nitrous oxide is analyzed by gas chromatography with an electron-capture detector (GC-ECD) and it is well known that low cost is one of its advantages compared to other techniques. This method has been used widely by a number of researchers over the past 20 years so there are many references on managing the analyzer. However, frequent calibration as running reference standards for this technique is strongly recommended to correct for the drift. The time taking to run samples (~4-6 mins per sample) is also suggested as a major disadvantage of this technique. The common method for CO is non-dispersive infrared (NDIR) absorption. It is convenient to measure CO continuously. However, frequent zero check is needed due to the drift. The NDIR method has a high detection limit so it is not suitable for the background levels of CO. Gas chromatography (GC) with a flame ionization (FID) detector or GC combined with a HgO reduction detector has advantages of good repeatability and low detection limits but they

are semi-continuous methods[3].

Recently, optical techniques based on laser-absorption spectroscopy for both gases were commercialized. One of those instruments, off-axis integrated cavity output spectroscopy (OA-ICOS), measures N_2O, CO and H_2O in the 4.6 μm regions with a tunable laser and an optical cavity (408 mL). This analyzer requires less maintenance at the station with continuous measurement based on seconds. Many previous studies have compared and demonstrated this new technique to previous analyzers; however, they were carried out inside laboratories or mainly in Europe[4][5]. Since all instrumental performance is dependent on local environment, it would be meaningful to show its performance in situ in Asian region station. The Korea Peninsula especially is affected by not only local sources/sinks but also outflows from the Asia continent, so it shows large fluctuations over a wide range with very distinct seasonal characteristics[6].

Here, we compared the conventional analyzers, such as GC-ECD and NDIR for N_2O and CO respectively, and OA-ICOS (Los Gatos, EP-40) that were installed at Jeju Gosan Suwolbong (JGS) GAW stations (126.16°E, 33.30°N, 71.47 m a.s.l.) for repeatability and linear response from March to July in 2018.

Sampling site and method

The JGS station is located in the west part of Jeju Island, which is the biggest volcanic island (1845.88 km^2) in the southwest of South Korea and about 90 km from the mainland. Jeju is popular with tourists regardless of the season, while the region of Suwolbong is famous as a global geopark due to the outcrops of volcanic deposits exposed along the coastal cliff where JGS is located. The side of the station from the southwest to the northwest is open to the sea, where there are volcanic basalt rocks. The sea to the south is connected to the East China Sea and the sea to the west is linked to the Yellow Sea. Next to JGS there is a wide plain where mainly potatoes, garlic and onions are harvested.

GC-μECD (Agilent 7890A) collects air from a 12 m height inlet and is calibrated by one working standard at a similar level to the ambient every 6 hours. These values are decided through the linear interpolations between successive calibrations. During one hour, we injected three times by the back-flush method. For NDIR, the air is sampled from a 9.5 m height inlet. The instrument is calibrated by zero and span (100.5 ppb) weekly while automatic zero checks are performed every 6 hours. Observed CO are decided through the linear interpolations between the calibrations and corrected by zero values.

OA-ICOS was installed next to the GC-μECD and also calibrated with one working standard fortnightly. The calibration correction occurs as a step–wise change. All sampled air is dried thorough cryogenic methods at -50℃ so the water vapor correction functions provided by the manufacturer are not applied.

Results

1. Precision test

Repeatability is defined as a precise measurement that is replicated with the same or similar objects over a short period of time and under a set of identical conditions, which includes the same measurement procedure, same operators, same measuring system, same operating conditions and the same location[7]. Meanwhile reproducibility is similar to repeatability such a measurement precision, however, under the condition, out of a set of conditions that includes different locations, operators, measuring systems, and replicate measurements on the same or similar object[7].

We categorized repeatability and short-term reproducibility factors. To test them, we sampled 4 working standards with different levels for an hour per cylinder with a sequence of A-B-A' over 7 hours. For this, we used 313.85, 335.85, 345.7 and 351.09 ppb for N_2O and 100.5, 102.4, 109.2, 207.9 and 465.2 ppb for CO. N_2O in cylinders has a traceability to WMO-X2006A while CO links to the KRISS (Korea Research Institute of Standards and Science) primary standard which is produced by the gravimetric method.

The repeatability is expressed as the standard deviation (1σ) of one hour while the short-term reproducibility means the drift changes during 7 hours. The ICOS repeatability and short-term reproducibility are in the WMO/GAW DQO for both N_2O and CO in Table 1 (compatibility goal for N_2O : ±0.1 ppb with ±0.3 ppb of extended value, CO: ±2 ppb with ±5 ppb of extended value). These values are quite similar to the previous studies for N_2O, 0.054 ppb, and for CO, 0.09 ppb, in hourly standard deviation[4][5].

For both GC and NDIR, only repeatability was similar to extended DQO, indicating the calibration frequencies should be on a hour. In this regard, ICOS has the advantage with stable and small drift compared to both techniques.

Table 1. The repeatability and short-term reproducibility assessment at JGS.

Analyzer	N_2O(ppb)		CO (ppb)	
	Repeatability (1 hour)	S-reproducibility (7 hours)	Repeatability (1 hour)	S-reproducibility (7 hours)
ICOS-EP40	0.03 (0.02-0.04)	0.07	0.06 (0.02-0.09)	0.09
GC	0.26 (0.20-0.36)	1.9	-	-
NDIR	—	—	5.2 (4.9-5.5)	11.8

2. Linearity test and calibration strategy

The calibration of test results is based on the premise that responses to instrument are linear in relation to the mole fraction of target species, or to reiterate, the sensitivities are the same within the range of mole fractions of interest. Our target range of N_2O is from 325 to 340 ppb and of CO from 50 to 500 ppb. For GC-ECD, it shows that the linear characteristic in the target range indicating the one-point calibration is enough when its value is similar to the target level. On the other hand, in this the responses of four standards are recalculated in consideration of equipment drift using the target tank injected bihourly. This means its drift is greater than the ICOS so that it should be considered the drift correction.

After NDIR is calibrated with zero (produced by filtering lab air) and span (100.5 ppb), it is used to measure the four standards. The measured data shows a non-linear relation to standards in the range of 50 to 500 ppb (Fig. 3). Residuals applying automatic manufactured linear fitting are increased as standards levels increase. On the other hand, residuals from the recalculated values by secondary polynomial formula are within the compatibility goal (±2 ppb).

We sampled one standard and used the calibration function provided by the manufacturer for the linearity test. For N_2O, we used 335 ppb and this covered the range of 310 to 345 ppb. However, it can be out of range of DQO when the level is over 345.7 ppb as indicated by the residuals increase as N_2O level increases (Fig.2). This result is similar to CO when we calibrated the instrument with one tank, 109.2 ppb (Fig.4). This suggests that the monitoring station in the region, which observes a wide range of atmospheric N_2O and CO like Korea, should be confirmed the covering range when the calibration function provided by manufacturer with one-point standard is used before monitoring atmospheric N_2O and CO.

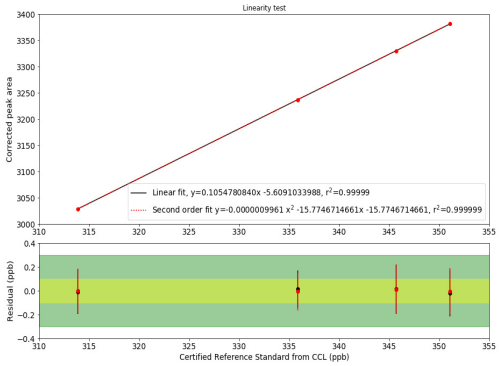

Figure 1

The linearity test of GC-ECD for N_2O. X-axis is standard tank and y-axis the instrument response (top). The residuals indicate the difference between theoretical value and observed value (bottom). The black line represents the linear function and the dots are the residuals between theoretical value from the linear function and observed values. The red lines and dots are derived from secondary polynomial formula.

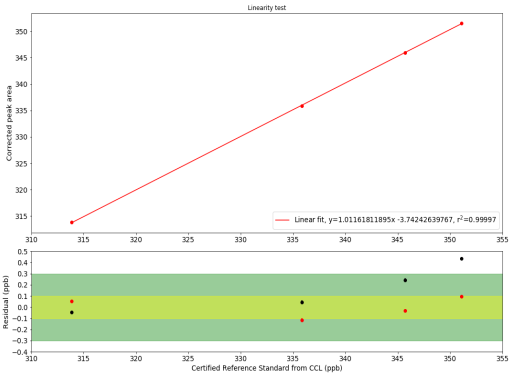

Figure 2

The linearity test of ICOS-EP40 for N_2O. X-axis is standard tank and y-axis the instrument response (top). The residuals indicate the difference between theoretical value and observed value (bottom). The black line represents the linear function and the dots are the residuals between theoretical value from the linear function and observed values. The red lines and dots are derived from secondary polynomial formula.

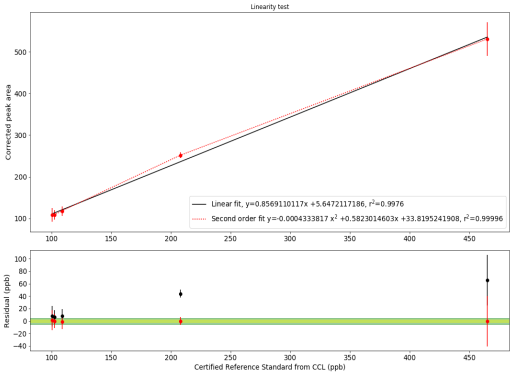

Figure 3

The linearity test of NDIR for CO. X-axis is standard tank and y-axis the instrument response (top). The residuals indicate the difference between theoretical value and observed value (bottom). The black line represents the linear function and the dots are the residuals between theoretical value from the linear function and observed values. The red lines and dots are derived from secondary polynomial formula.

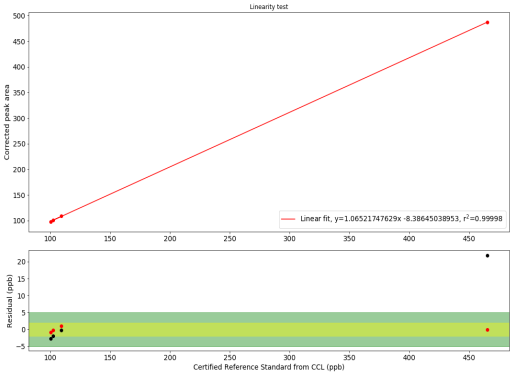

Figure 4

The linearity test of ICOS-EP40 for CO. X-axis is standard tank and y-axis the instrument response (top). The residuals indicate the difference between theoretical value and observed value (bottom). The black line represents the linear function and the dots are the residuals between theoretical value from the linear function and observed values. The red lines and dots are derived from secondary polynomial formula.

Summary

From 1 March to 20 July in 2018, we compared the new technique of OA-ICOS to the conventional methods of GC-ECD and NDIR for N_2O and CO, respectively. Through the precision and linearity test, GC-ECD should correct the drift through the injection of target tank bihourly and decide the number of standard tanks for calibration after assure the linear characteristic. NDIR should be calibrated with at least three points covering the range of interest (for example, around 100 ppb, 200~400 ppb, 500~1000 ppb) and data is needed to compensate zero drift and recalculate by secondary polynomial calibration formula.

This comparison shows ICOS has a better repeatability and less drift performance than the conventional technique. One-point calibration using the calibration formula provided by the manufacturer cannot cover the whole range such that it should be confirmed by the range assured by it. In the future, zero test and long-term reproducibility should also be implemented to get a better calibration strategy.

Acknowledgments

This work was funded by the Korea Meteorological Administration Research and Development Program "Research and Development for KMA Weather, Climate, and Earth system Services– Development of Monitoring and Analysis Techniques for Atmospheric Composition in Korea" under Grant (KMA2018-00522)

Reference

[1] Alexander et al., (2013): Climate Change 2013. The physical science basis. Intergovernmental panel on climate change, working group Ⅰ contribution to the IPCC fifth assessment report, Cambridge University Press.

[2] Myhre et al., (2013): Climate Change 2013. Chapter 8. Anthropogenic and Naatural Radiative Forcing

[3] GAW Report No. 192(2010), Guidelines for the Measurement of Atmospheric Carbon Monoxide

[4] Lebegue et al., (2016): Comparison of nitrous oxide (N_2O) analyzers for high-precision measurements of atmospheric mole fraction, Atmos. Meas. Tech., 9, 1221-1238

[5] Zellweger et al., (2012): Evaluation of new laser spectrometer techniques for in-situ carbon monoxide measurements, Atmos. Meas. Tech., 5, 2555-2567

[6] Lee et al., (2019): The measurement of atmospheric CO_2 at KMA GAW regional stations, its characteristics, and comparisons with other East Asian sites, Atmos. Chem. Phys., 19, 2149-2163

[7] JCGM: International vocabulary of metrology-

Basic and general concepts and associated terms (VIM, 3rd edition, 2008 version with minor corrections), available at: https://www.bipm.org/utils/ common/documents/jcgm/JCGM_200_2012.pdf (last access: 20 March 2019), 2012.

A Detachable Trap Preconcentrator with GC-MSD for the measurement of Trace Halogenated Greenhouse Gases

Doohyun Yoon[1,2], Jeongsoon Lee[1*], Jeong Sik Lim[1*]

1. Center for gas analysis, Korea Research Institute of Standards and Science (KRISS), Gajeong-ro 267, Yuseong-gu, Daejeon, 34113, Republic of Korea
2. Department of Measurement Science, University of Science and Technology (UST), Gajeong-ro 217, Yuseong-gu, Daejeon, 34113, Republic of Korea

Introduction

In this study, a preconcentration system for GC-MS will be presented, which is empowered by a detachable trap for the quantitative analysis of NF_3 and other trace fluorinated gases with high precision. The cooled preconcentration trap was separated from the cold-end of the cryogenic refrigeration unit during heating for desorption of the preconcentrated analytes, thereby restricting the heat transfer to the cold-end and secondary trap. Thus, the system steadily maintains the ground-state temperature of the base plate at approximately −135°C, thereby improving the cooling rate of the heated trap compared to that in the integrated configuration. A preconcentration of NF3 in a matrix of air at −135°C is demonstrated by fully custom-built preconcentration system with high measurement precision.

Experiment

1. Gas line configuration

The gas plumbing consists of multiposition valves (Valco Instrument Company Inc.), mass flow controller (MFC, 5850E, Brooks Instruments), flow meters, helium purifier, electric pressure controllers (EPC), two adsorptive traps, split inlet, precolumn, and main column. (Figure 1) The temperature controller (TM4, Autonics) communicated with the PLC via the RS-485 protocol and used the solid-state relay (SSR, 24 VDC, LSIS) to control the temperature of

the heater cartridge through the Proportional–Integral–Derivative (PID) control. The actuator control is divided into a solenoid valve control using air pressure and a multi-position valve driver control. V1, V2, V3, V4, and linear motions are controlled in two states, on and off. The EPC and the inlet, both of which are capable of controlling the flow rate of the analyte stream, were installed in the GC (Agilent 7890) body and controlled by the GC control program. T1 and T2 are adsorptive traps consisting of stainless steel tubes with an inner diameter of 2.18 mm and length of 100 mm. T1 (concentrating trap) and T2 (refocusing trap) were filled with 120 mg and 10 mg, respectively, of Hayesep D (100/120 mesh, Valco Instruments). The temperature of the traps could be controlled stably at designated temperature between −135°C and 0°C over ~5 min, thereby determining the type of gas desorbed. A differential trapping method was applied to remove decent portion of major interfering substances such as CO_2, N_2, and O_2 in order to ensure sufficient sampling volume of T2. The gas was adsorbed in T1 that was maintained at the -135°C, and then the temperature of T1 was set to −75°C for selective desorption of a significant amount of CO_2 that could be vented out. This was accomplished without using any CO_2-removal agent such as the Molecular Sieve adsorbents, so which allowed for the strong retention and back-flushing of CO_2. Residual CO_2 was chromatographically separated in the main column of Porabond Q (length, 75 m; i.d., 530 μm; film thickness, 10 μm; Varian Inc.). The precolumn (stainless steel, internal diameter: 2.18 mm, length: 30 cm) was filled with 50 mg of 100/120 mesh molecular sieve 4 Å (MS 4 Å, Sigma Aldrich) and then with 200 mg of 100/120 mesh HiSiv-3000 (Hisiv, UOP). The MS-4A/HiSiv-3000 mixed precolumn was used to separate CF4 from interfering gases such as N_2, O_2, Ar, Kr, CH_4, and CO_2. In particular, an excess of CO_2 was back-flushed by the aid of strong retention in MS-4A. However, in case of measuring NF_3, the precolumn was bypassed from the flow path owing to the NF3 removal characteristics of HiSiv-3000. The interference by CO_2 resulting from the bypass of MS-4A was solved by partial venting, the efficiency of which was determined by the transfer temperature. Details regarding operation sequences and their strip chart are given in [1].

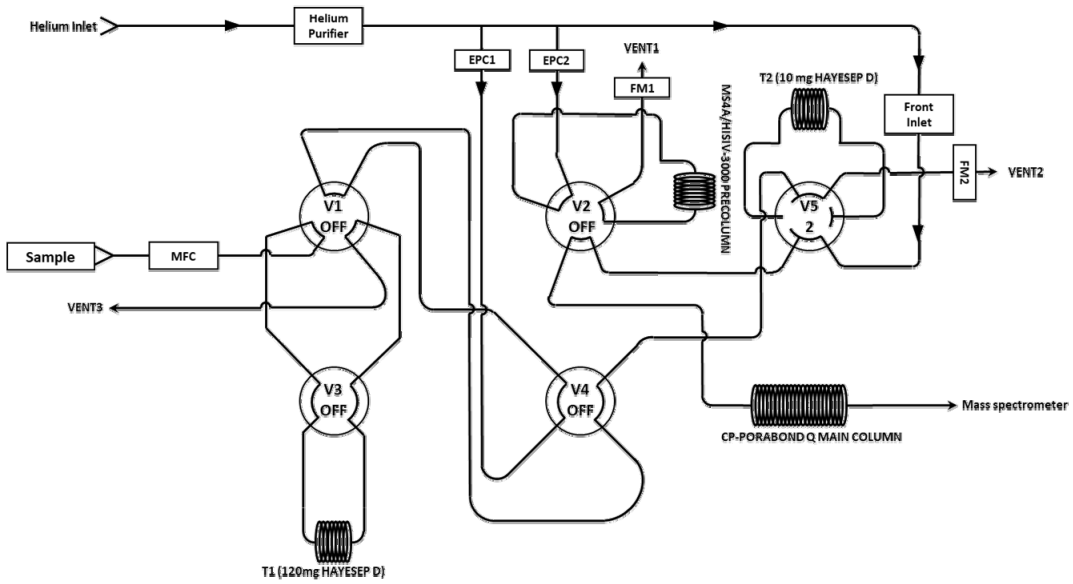

Figure 1

Schematic illustration of gas line configuration of the developed detachable trap preconcentrator-GC/MS system. The five multiposition valves are referred to as V1, V2, V3, V4, and V5, and the traps are referred to as T1 and T2. The carrier gas He is refined and then allowed to flow through the purifier, and its flow rate is controlled by the electric pressure controllers (EPC1 and EPC2). The flow rate of the sample is adjusted by the MFC and is located in upstream of T1. A combined precolumn sequentially filled with MS-4A and Hisiv-3000 was used to separate CF_4 and analytical interfering substances before the analyte is transported to the main columnat T2. For measuring NF_3 the combined precolumn was bypassed in order to avoid the removal of NF_3 by Hisiv-3000. CO_2 was selectively desorbed in T1, whose temperature was tuned at −75°C, and then vented out before transferring T2. Flow meters are referred to as FM1 and FM2

2. Detachable trap

A cold-end (PT-14, Polycold Division of Brooks Automation, Petaluma) connected with a high-performance cryogenic refrigeration unit (Cryotiger, Polycold Division of Brooks Automation, Petaluma) was used as a cooling unit for the detachable adsorption traps. The cold-end used in this study has a cooling capacity of 30–50% at −160°C compared to that of PT-16 used in Miller's work.2 Though, in our work, the ground-state temperature of the baseplate could be down to −145°C, it was maintained at -135°C during continuous measurements. To minimize heat transfer between the trap and the freezer, the copper baseplate buffered thermal flow by being placed between the cold end and the trap. In case of that T1 and T2 shared the baseplate, the temperature of T2 was gradually increased at the rate of ~10°C/min by the T1 at −65°C. Therefore, in order to minimize the thermal exchange between T1 and T2, the baseplates of those were divided into two parts. (Figure 2) Each baseplate (dimensions, 15 × 7 × 40 mm) has two grooves for tight contact between the straight adsorptive tube and welded cartridge heater, where thermocouples are welded on the rear side of the baseplate. Nevertheless, the

temperatures of two traps were affected by each other when attached simultaneously in the base plate. Since the temperature deviation induced by another trap strongly hinders to take precision control of adsorption amount of target analytes, it was essential to improve a temperature isolation of two traps. For this, the trap was physically detached by air-actuated linear motions (L-2171-1, Huntington Mechanical Labs) when if the temperature was increased higher than 0°C. Cooling to the background temperature or maintaining a moderate temperature, the trap is pushed toward the baseplate and attached-on. A polymer union placed between the arm of the linear motion and the trap served to block incoming and outgoing heat through the linear motion. In this way, even when the trap is heated to 200°C, the temperature of the base plate can stay at the background level of -135°C, and therefore sufficient cooling power is provided for quick cooling. Though, the reattachment of the T1 to be cooled impulsively increased T1 temperature (~22 min), this is trivial to the measurement precision because of no gas flow between T2 and the GC-MS. Note that consecutive injection of NF3 followed by HFCs within one cycle is required for T1 to be maintained at −75°C during first injection-heating and cooling-down of T2 as in Miller's study.2 This requirement might be fulfilled by ensuing higher cooling power.

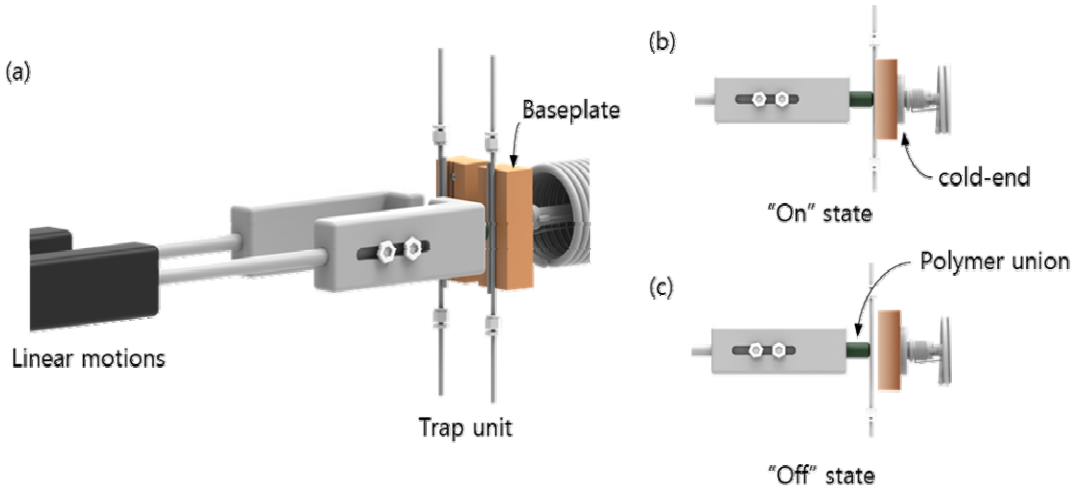

Figure 2

View of the detachable preconcentration traps. (a) The baseplate is divided into two parts for blocking heat transfer from another trap that is heated. There are two grooves for tight attachment of the trap unit of adsorbent line and heat cartridge, where thermocouples are welded on the rear side of the baseplate. The trap unit is connected to the arm of the linear motion spaced by a polymer union, which serves to block incoming and outgoing heat through the linear motion (b) "On" state. When cooling or maintaining a moderate temperature, the trap is pushed toward the baseplate and attached-on. (c) "Off" state. The linear motion pulls the trap for heating to high temperature. This structure is registered in Korean Patent No. 1017078640000.

Results and discussion

1. The impact of the trap temperature on the chromatographic resolution

In order to remove CO_2, which is the most interfering substance during the measurement of NF_3, the temperature of T1 was set close to the sublimation point of CO_2 during the transfer of analytes from T1 to T2. The area of the NF3 peak remained the same regardless of the transfer temperature ranging from −75 to −50°C. However, in the case of transferring at −50°C, the chromatographic resolution decreased compared to that of −75°C. This phenomenon might have resulted from the considerable retention by the adsorbent Hayesep D in T1. In order to achieve sufficient refocusing power of T2, reducing the amount of the adsorbent can be considered, however, a compromise is needed to minimize the adsorption loss. Alternatively, CO_2 should be completely removed by back-flushing in the precolumn or by using a chemical trap such as lime soda before preconcentration. Step 8 in the measurement of NF_3 and HFCs involves refocusing and the temperature of T2 was maintained at a high value with the closure of T2. In this step, the delayed retention time and tailing phenomena caused by the interaction between stationary and mobile phases at T1, precolumn, and T2, can be improved by a long dwelling time of Step 8. This is because a uniform temperature distribution from the trap surface to the core might be derived by long dwelling time at T2. Prolonging Step 8 for more than 5 min improved the peak shape to be symmetric, suggesting repeatable peak integration, namely detection response.

2. Ambient air measurement

The total ion chromatogram of a trace HFC mixture was reconstructed from independent acquisitions of chromatograms over sixty m/z units. (Figure 3) For this purpose, the three independent chromatograms were recorded in SIM (selected-ion monitoring) mode at m/z values covering 10~69, 70~129, and 130~189. In post-processing, chromatograms obtained at m/z = 28, 32, 44, 18, 14, 16, and 17 corresponding to N_2, O_2, CO_2, H_2O, N, O, and OH, respectively, were discarded. The last chromatograms were combined to yield the reconstructed total ion chromatogram (TIC). The side-peak of the major abundant N_2 corresponding to m/z = 29 was also blind-treated. Their chemisorption on the Hayesep D should be poor; however, physisorption caused by low-temperature cooling at −135°C allows a considerable amount of these components to be concentrated and then injected into the mass spectrometer along with the analytes. These physisorbed components, which account for 99.07% of ambient air, were excessively injected and remained in the source region to

be ionized. In this sense, the side band of CO_2 (m/z = 45) and N_2 (m/z = 29) indicated that excessive amounts of parent ions with m/z = 29 and 44 leaked through the mass filter to reach the detector. Evidently, the response of the corresponding m/z in the chromatogram was consistent (>30000) for ~10 min after injection, implying continuously leaked (or unfiltered) ion current. Unless they are discarded, the baseline of the TIC is saturated to blind the peaks where various analytes are separated.

Dry air collected in pressurized aluminum cylinders in August 2015 at Anmyeondo (AMY), Republic of Korea, was analyzed. By contrast to the NIST 2008 mass library, HFO-1234yf (CH2CFCF3) and HFO-1243zf (CH2CHCF3), which are increasingly used as the fourth-generation refrigerants, were newly identified in the sampled dry air. (Figure 4) In the case of HFO-1234yf, the mass spectrum was verified by measurement of the commercially available raw gas (Opteon YF, Chemours company, USA) diluted with nitrogen. Qualitative assignments of the other unknown peaks will be obtained in the near future. Additionally, dry air samples archived in 2006, 2011, and 2015 at Gosan, Republic of Korea, were analyzed to compare the results with the AGAGE-reported observation values for NF_3, HFC-134a, HCFC-22, and HCFC-142b at Zeppelin.8

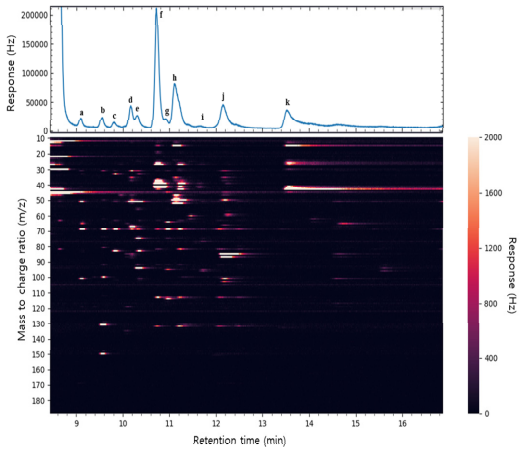

Figure 3

Mass spectrum according to the retention time of the total ion chromatogram (TIC) (top) and analytes (bottom); m/z = 14, 16, 17, 18, 28, 29, 32, and 44 were blinded with a high baseline for easy identification of the peaks (see text). a: PFC-218 (CF_2CFCF_2) and HFC-143a (CH_3CF_3), b: Hexafluoropropylene ($CF_3CF=CF_2$), c: HFC-134a (CH_2FCF_3), d: HCFC-22($CHClF_2$), e: Combined peaks of 3, 3, 3-trifluoropropyne (CF_3C_2H) and HFC-245ca ($CH_2FCF_2CHF_2$), f: Propene ($CH_3CH=CH_2$), g: HFO-1234yf ($CH_2=CFCF$), h: Chloromethane (CH_3Cl), I: HFC-1243zf ($CH_2=C_2HF_3$), j: CFC-12 (CCl_2F_2), and k: HCFC-142b ($C_2H_3ClF_2$)

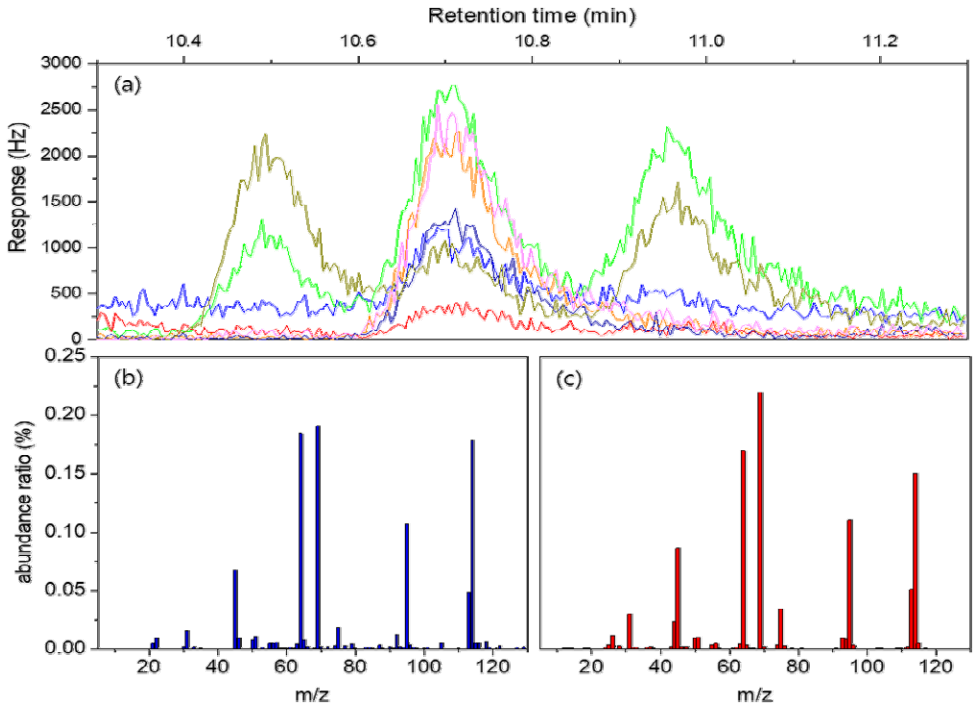

Figure 4

(a) Chromatograms of HFO-1234yf (CH_2CFCF_3) of dry air sample peaked at 10.7 min. Chromatograms are taken at m/z=45(blue), 64(orange), 69(green), 75(red), 95(violet), 113(darkyellow), and 114(magenta). (b) The NIST mass spectrum library of HFO-1234yf and (c) measured mass spectrum of a diluted HFO-1234yf raw gas are also represented. $C_3H_2F_4^+$(114), C_3HF4^+(113), $C_3H_2F_3^+$(95), $C_3HF_2^+$(75), CCF_3^+(69) and $C_2H_2F_2^+$(64), and CH_3CF^+(45) were identified in both mass spectra.

Conclusion

An ultralow-temperature preconcentrator coupled with a GC-MS system was developed for measuring various trace greenhouse gases such as NF3 and HFCs, which are rapidly increasing in the modern atmosphere. For the efficient elimination of the major components of air, the differential adsorption traps equipped with Hayesep D were cooled at -135°C before the injection of the analyte sample into the GC-MSD. The transfer temperature of the primary adsorption trap, T1, was adjusted to −75°C for efficient desorption of CO_2 (one of the major interfering substances of NF_3/CF_4), and significant ventilation was induced to secure sufficient sampling volume in the refocusing trap, T2. This approach presents the possibility of bypassing the use of back-flushing. In particular, it is an essential process for the detection of NF_3, considering that NF_3 is highly adsorbed onto the Hisiv 3000. Linear motions were used to detach the traps from the

freezer, thereby limiting heat transfer to the freezer to maintain the baseplate in the ground state temperature of −135°C. This strongly implies that NF_3 can be detected by GC-MSD under mild temperature conditions in the preconcentrator and suggests further improvement of the LOD and measurement precision. This trap design might effectively overcome the insufficient cooling capacity.

We demonstrated that NF_3 and HFCs at the background atmospheric level levels can be measured with precisions of 0.35% at the rate of 35 min/cycle and 0.35% at 45 min/cycle, respectively. NF_3 was measured by diluting 5 pmol/mol NF_3 in air (prepared via the gravimetric method) with N_2. A linear response was observed within 0.5% up to 0.51 pmol/mol, and the LOD was estimated to be 0.21 pmol/mol. Based on these results, we aim to establish a calibration scale for the measurement of gases by developing a highly precise NF_3 standard using the gravimetric method.

Reference

[1] Yoon et al. (2019): Detachable trap preconcentrator with a gas chromatograph-mass spectrometer for the analysis of trace halogenated greenhouse gases, Anal. Chem., 91 (5), 3342-3349

[2] Arnold et al. (2012): Automated measurement of nitrogen trifluoride in ambient air, Anal. Chem. 84 (11), 4798-4804

GHGs measurement from aircraft in India

Yogesh K. Tiwari*, Smrati Gupta

Indian Institute of Tropical Meteorology, Pune, India

Introduction

Atmospheric CH_4 is known to be the second most important greenhouse gas with lifetime approximately 12 years, radiative forcing 0.97 Wm^{-2}, and global warming potential 25 times higher than CO_2. Methane has both natural (wetland and termites)[1],[2] and anthropogenic sources (rice cultivation, landfills, fossil fuel)[3],[4]. Atmospheric CH_4 reacts with OH radicals and affects oxidizing capacity of the atmosphere as well as affects ozone and water vapor levels in the stratosphere[5]. South-East Asia is considered to have big source of CH_4 mainly due to wetlands, livestock, waste management, and various other anthropogenic activities [6],[7]. India is a second largest CH_4 emitter in the world due to anthropogenic and natural sources [7]. Atmospheric CH_4 observations in India are mainly focused on surface monitoring sites[8],[9],[10],[11],[12] as well as satellite retrievals and commercial airplane observations [13],[14]. CARIBIC aircraft campaigns studied upper tropospheric CH_4 and other GHGs using commercial airliner[15],[16]. They reported enhancement of CH_4 during summer monsoon months near Indian continent (south of 40^o N latitude) and between altitudes 8 to 12.5 Km.

CH_4 emissions in India peaks during Indian summer Monsoon (ISM) months whereas seasonal cycle of surface CH_4 mole fraction observations peaks during winter months and dips during ISM months[11]. ISM season witnesses higher CH_4 emissions mainly due to rice paddies and wet lands, while due to strong deep convection surface CH_4 emissions from various sources, along with other pollutants, are transported vertically and distributed within lower to upper troposphere[17],[15],[11]. On the contrary, vertical transport due to deep convection is absent during winter months.

Overall, observational efforts are mainly centered either at the surface, upper troposphere, or satellite retrievals. Three-dimensional general circulation models suggest that the vertical gradient of CH_4 is a product of competing source and sink terms coupled with atmospheric mixing processes18. Satellites have capability to monitor column averaged CH_4 vertical distributions[19],[20] but most of the satellites retrievals have limited capacity and there is huge observational gap due to persistent clouds during ISM months over India[21]. In a separate study an airplane campaign conducted over Bhubaneshwar, Varanasi, and Jodhpur area in India for one month during June 2016 and showed the variability of GHGs from surface to 3.2 km[22]. There is no study available above boundary layer using aircraft measurements.

In this study, first time, we present vertical structure of atmospheric CH_4 level over India observed by aircraft. Also, this study discusses about observations of vertical profiles and large scale transport processes and tropospheric variability of atmospheric CH_4 using airplane campaigns during September and November 2014 and July 2015 over India.

Methods

Instrumented aircraft beechcraft super king twin engine aircraft B200 were used to conduct campaigns during Sept. 2014, Nov. 2014 and July 2015. In this section we described about study area, Aircraft attained maximum altitude of 8 Km. Figure 1 demonstrates CAIPPEX flight paths over Varanasi (VNS; Sept. 2014), Mahabaleshwar (MBL; Nov. 2014), and Kolhapur (KHP; July 2015). CH_4 (ppb) mole fraction were monitored using Cavity Ring Down Spectroscopy (CRDS) technique based instrument. This instrument is specially designed for aircraft measurements consisting external pump which maintains air sample pressure at all altitudes during the flight. Apart from CRDS various other instruments were used for atmospheric monitoring as well as time-synchronized latitude, longitude, altitude etc. Reverse facing air sample inlet was connected to CRDS instrument with 140 cm quarter inch size (OD) swagelok tubing. The cruising altitude of aircraft rages from surface to 8 km.

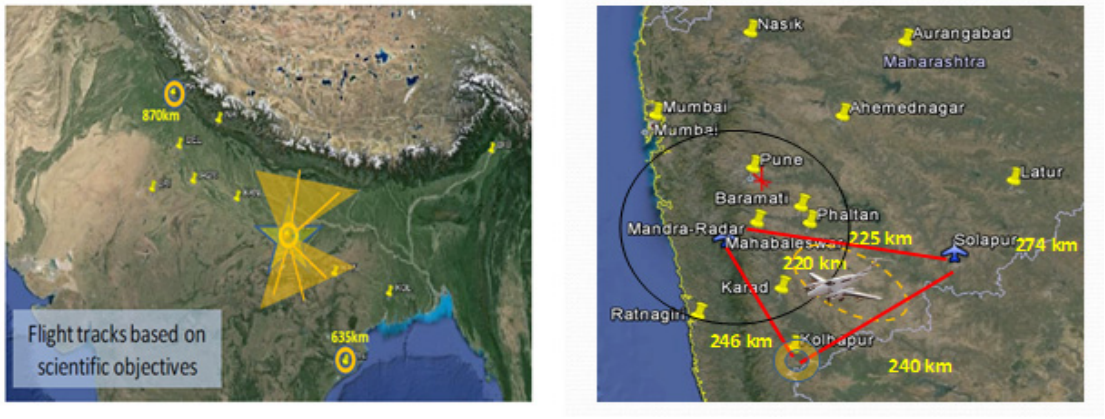

Figure 1

Aircraft observations locations over India, during Sept. & Nov. 2014 (left panel) and July 2015 (right panel)

1. Instrument

We used Cavity Ring Down Spectroscopy (CRDS) instrument from Picarro Inc. USA (flight analyzer G2401-m) to monitor CH_4. CRDS is connected to reverse inlet (inlet looking opposite to the aircraft flying direction) to avoid any direct contamination in the inlet line and supply continuous airflow to the instrument. Water vapour corrected dry mole fraction of CH_4 (ppb) are monitored in ambient atmosphere during the flight. Atmospheric CH_4 is less affected by varying water vapour in the atmosphere [26].

CRDS system comprises of main equipment i.e. analyzer and a pumping unit. The analyzer is equipped with number of fixed lasers, a high precision wavelength monitor, an optical cavity, high reflectivity mirrors (>99.995%) inside cavity, a photodetector and a computer [26]. Once air sample is filled inside cavity during measurement, laser light at a specific wavelength injected into the cavity through a partially high reflective mirrors and the light intensity which builds up over time is detected and measured through a second partially high reflecting mirror using a photodetector located outside the cavity. Lasers are rapidly turned off and ring-down time are measured by measuring time constant of the light intensity as it exponentially decays. Analyzer was developed specifically for aircraft measurements. Since atmospheric pressure variation in the upper atmosphere are totally different than the surface, aircraft analyzer was fitted with other specific equipments such as an ambient pressure sensor (with pressure correction to wavelength monitor so that wavelength targets are achieved under fast changing atmospheric pressure), additional temperature sensors (for analyzers temperature control system in changing atmospheric pressure), a solid state computer drive, and higher data acquisition

rate. In flight analyzers, cavity pressure depends on sampling gas flow in pressure changing ambient environment, mechanical vibration during the flight operations. We have investigated monitored cavity pressure of each flight and found it very stable (close to 140 millitorr, figure not shown). It indicates that analyzer was very much stable during the flight operations. More detailed description of the analyzer and its basic development by scientific community is published [26].

2. Calibrations

Calibration standards which are used during aircraft observation are traceable to the WMO standard scale and were imported from NOAA Boulder Colorado USA. Three standard tanks at NOAA-X2004 scale were connected to CRDS instrument consecutively for 20 minutes each and last 15 minutes of data were utilized for calibration of flight observed values. Calibration tanks were measured before takeoff and after landing only. No calibration was done during the flying hours because of permissions issues on flying of high pressure cylinders. Figure 2 demonstrates three point calibration curve and a vertical profile of cavity pressure of one of the flights. Cavity pressure is almost constant with the altitude which shows that instrument was stable while flying and output data is reliable.

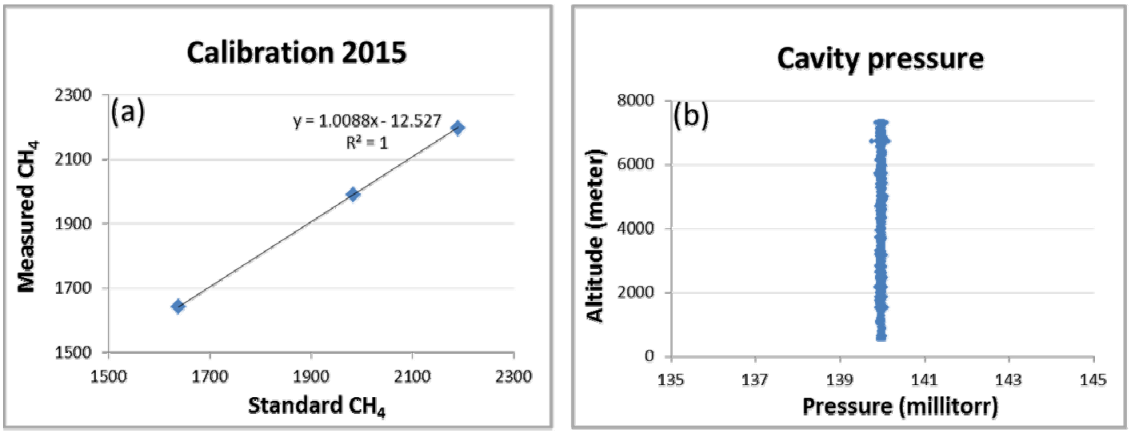

Figure 2

(a) Calibration curve and (b) Cavity pressure profile of randomly selected day during aircraft campaign, measured by Picarro 2401-m

Results and Conclusions

Figure 3 (a) (b) (c) represents aircraft vertical profiles observed during July 2015 over Kolhapur (KHP) India, September 2014 over Varanasi (VNS) Ganga Basin India; and November 2015 over Mahabaleshwer (MBL) India; respectively. Mean CH_4 of all the profiles is represented by the solid lines and color bar represent number of flights during respective campaign period. CH_4 is higher at the surface over VNS and gradually decreases with the height. VNS is densely populated area, situated over Ganga Basin and significantly contributes CH_4 emissions to the atmosphere. CH_4 mole fraction varies between 2100 – 2300 ppb at the surface, 2000 ppb at the lower atmosphere (< 2 Km), and 1900-1950 ppb at the middle troposphere (5-7 km). MBL is located western part of India where observed CH_4 level at the surface is higher than middle and upper tropospheric values. In contrast with these, CH_4 mole fraction at KHP is lower at the surface and increases with height.

Figure 3 (d) (e) (f) represents Laboratoire de Météorologie Dynamique (LMDZ) model simulated CH_4 profiles as the same time and location as the aircraft observations. Zoomed version of LMDZ with horizontal resolution of 0.51x0.66 (latitude by longitude) and 39 sigma pressure vertical levels over Indian region are validated extensively with the surface CH_4 observations over India [12]. Model was simulated during years 2000-2015 and first six years are considered as a spin-up time. This model utilizes combination of surface fluxes to simulate CH_4 fields during the prescribed period. For example, anthropogenic emissions are taken from EDGAR v4.2; emissions from rice cultivation are from [23] wetland emissions is based on [24] etc. Model uses ECMWF reanalysis meteorological field at 6-hour interval to drive the fluxes. Details of model and prescribed fluxes are available in [12].

Figure 3 (g) (h) (i) represents The Center for Climate System Research/National Institute for Environmental Studies/Frontier Research Center for Global Change (CCSR/NIES/FRCGC) atmospheric general circulation model (AGCM) based CTM (ACTM)[25] simulated CH_4 profiles as the same time and location as the aircraft observations. The horizontal resolution of ACTM is $2.8^o \times 2.8^o$ latitude by longitude with 67 pressure-sigma layers in the vertical.

Observations and models agree very well. Few of the flights simulated by both LMDZ and ACTM are exactly matching (e.g. profile represented by dark brown color solid line). During summer monsoon months (JJAS) over India strong vertical transport occurs due to convection. In such case pollutants and gases gets carried away in the upper atmosphere under the influence of the vertical convection. As aircraft observed CH_4 mole fraction over

Varanasi is high at the surface, it gets transported to lower and middle troposphere due to high convection. Once it reaches middle troposphere it is again trapped in already existing easterly flow and moves towards the south-west direction (Figure 4 and Figure 5). Observed CH_4 level at Kolhapur during July month is low at the surface and increase with height and peaks at middle troposphere (4 to 5 km). CH_4 mole fraction vertically transported from Varanasi Ganga Basin and moved towards south-west due to easterly flow, is a similar magnitude CH_4 signal observed at middle troposphere over Kolhapur. Therefore we assume that there is strong vertical transport over Varanasi Ganga Basin which carries surface CH_4 emissions towards middle troposphere and it further moves towards south-west direction (towards Kolhapur) due to easterly jet. Both observations and models show similar feature which gives more confidence on this hypothesis. But we need more observations and improved high resolution modeling to ascertain these results. These observations will be very useful in understanding greenhouse gases three dimensional moment over the Indian region during summer monsoon months.

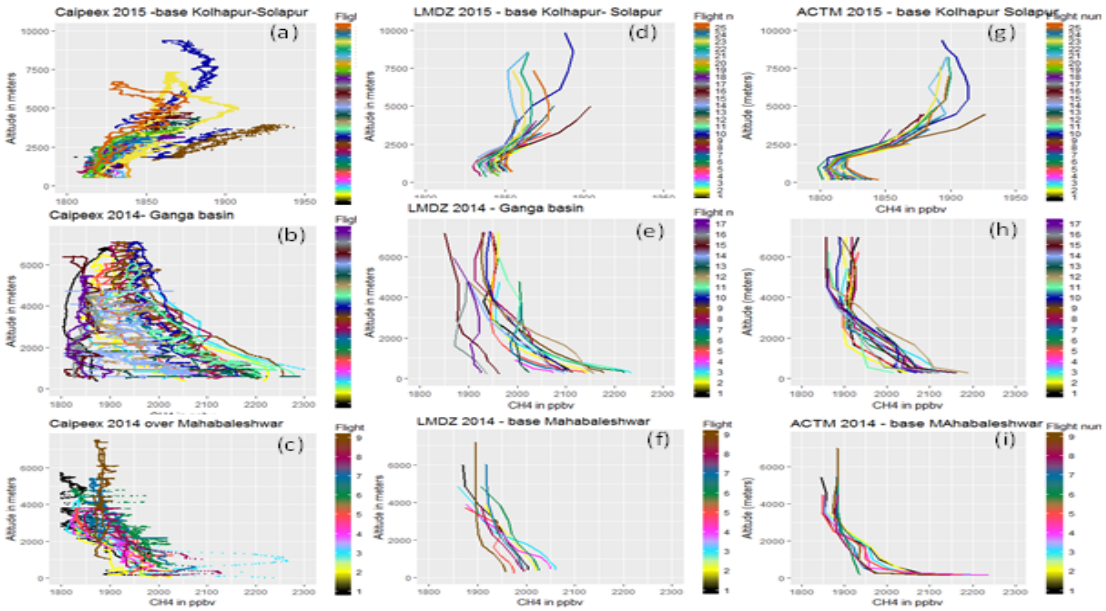

Figure 3

(a-c) CH_4 (ppb) observations measured by aircraft during July 2015 over Kolhapur, Sept. 2014 over Varanasi Ganga basin, and Nov. 2014 over Mahabaleshwar. (d-f)) LMDZ model simulated CH_4 and (g-i) ACTM model simulated CH_4 Color bar represents total number of flights.

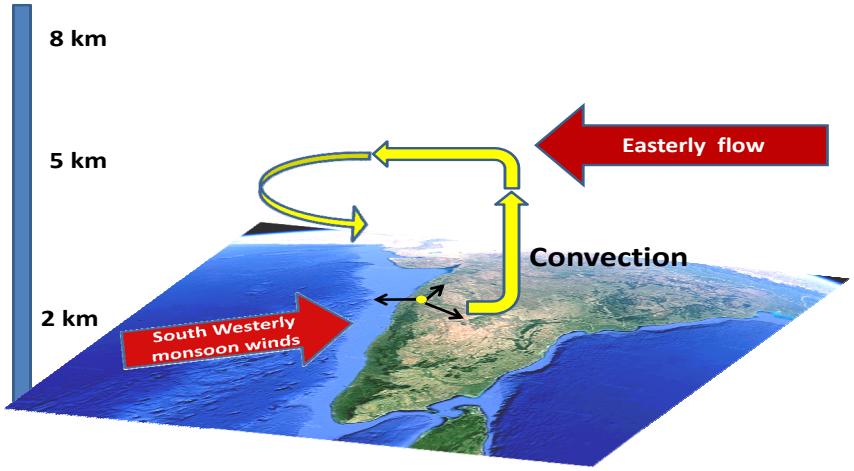

Figure 4

A typical schematic showing vertical transport due to strong convection and easterly flow at mid-troposphere during summer monsoon months over India.

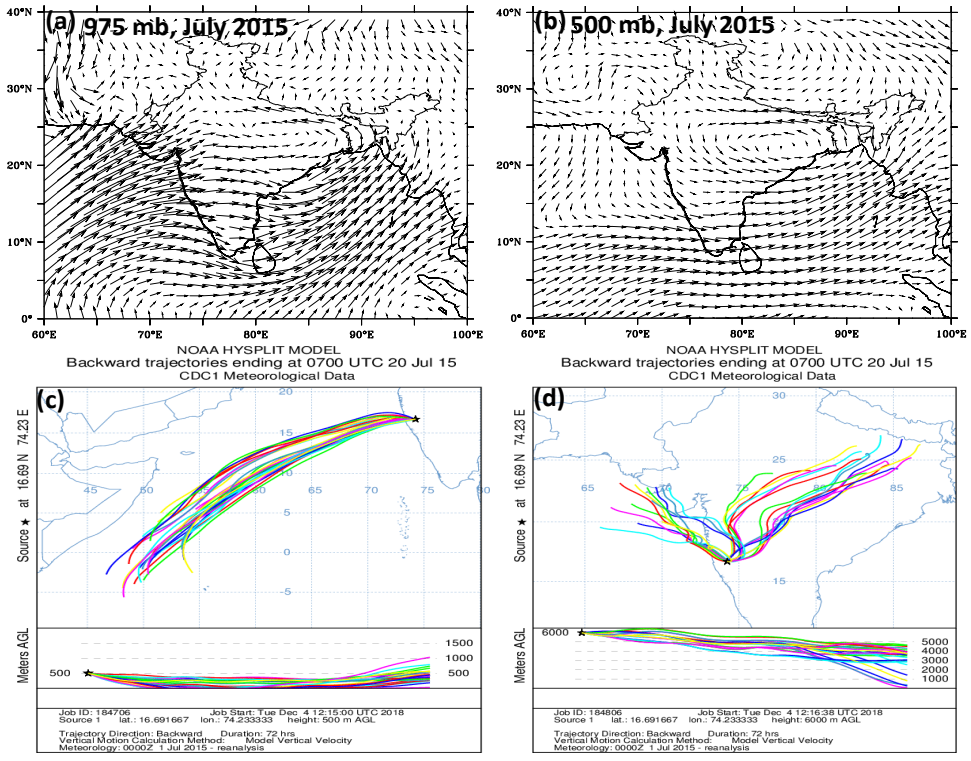

Figure 5

(a-b) Wind vectors at 975 mb and 500 mb during July month over India, (c-d) 7-day backtrajectory at surface and middle troposphere originates from Kolhapur during July month.

Acknowledgments

Authors would like to thank Dr. Thara Prabhakaran, Chief of CAIPEEX project and entire CAIPPEX team for their enormous support and encouragement for conducting GHGs airplane observations. Also, we would like to thank Director IITM Pune and Ministry of Earth Sciences Govt. of India for providing financial support for this experiment.

Reference

[1] Cao et al. (1998): Global methane emission from wetlands and its sensitivity to climate change. Atmos. Environ. 32 (19), 3293e3299. http://dx.doi.org/10.1016/S1352-2310 (98) 00105-8.

[2] Sugimoto et al. (1998): Methane oxidation by termite mounds estimated by the carbon isotopic composition of methane, Global Biochemical Cycles. Vol.12 (4) 595-605

[3] Crutzen et al. (1986): Methane Production by Domestic Animals, Wild Ruminants, Other Herbivorous Fauna, and Humans. Tellus B. 38B. 271 – 284. 10.1111/j.1600-0889.1986.tb00193.x.

[4] Oliver et al. (2006): Recent trends in global greenhouse gas emissions: regional trends and spatial distribution of key sources. Non-CO_2 Greenhouse Gases (NCGG-4).

[5] Lelieveld et al. (1998): Changing concentration, lifetime and climate forcing of atmospheric methane, Tellus,Ser.B,50,128-150,1998

[6] Bergamaschi et al. (2009): Inverse modeling of global and regional CH_4 emissions using SCIAMACHY satellite retrievals 17 November 2009 https://doi.org/10.1029/2009JD012287

[7] EDGAR (2014): European Commission, J. R. C. (JRC)/Netherlands E. A. A. (PBL). Emission Database for Global Atmospheric Research (EDGAR), release EDGARv4.2 FT2012, available at http://edgar.jrc.ec.europa.eu.

[8] Bhattacharya et al. (2009): Trace gases and CO_2 isotope records from Cabo de Rama, India. Curr Sci. 97(9), 1336–1344.

[9] Tiwari et al. (2011): Glass flask air sample analysis through gas chromatography in India: implications for constraining CO_2 surface fluxes, WMO/GAW Report No. 194, WMO/TD-No.1553

[10] Tiwari et al. (2014): Influence of monsoons on atmospheric CO_2 spatial variability and ground-based monitoring over India, Science of The Total Environment. 490 (15), 570–578, http://dx.doi.org/10.1016/j.scitotenv.2014.05.045.

[11] Tania et al. (2017): What controls the atmospheric methane seasonal variability over India?,Atmospheric Environment, 175,

83–91, https://doi.org/10.1016/j.atmosenv.2017.11.042

[12] Lin et al. (2018): Simulating CH_4 and CO_2 over South and East Asia using the zoomed chemistry transport model LMDzINCA. Atmos. Chem. Phys., 18, 9475-9497, 2018, https://doi.org/10.5194/acp-18-9475-2018

[13] Kavitha et al. (2016): Region- dependent seasonal pattern of methane over Indian region as observed by SCIAMACHY. Atmos. Environ. 131, 316e325. http:// dx.doi.org/10.1016/j.atmosenv.2016.02.008.

[14] Kavitha et al. (2016): Non- homogeneous vertical distribution of methane over Indian region using surface, aircraft and satellite based data. Atmos. Environ, 141, 174-185.

[15] Schuck et al. (2012): Distribution of methane in the tropical upper troposphere measured by CARIBIC and CONTRAIL aircraft. J. Geophys. Res. 117, D19304

[16] Schuck et al. (2010): Greenhouse gas relationships in the Indian summer monsoon plume measured by the CARIBIC passenger aircraft, Atmos. Chem. Phys., 10(8), 3965–3984, doi:10.5194/acp-10-3965-2010

[17] Patra et al. (2011): TransCom model simulations of CH_4 and related species:linking transport, surface flux and chemical loss with CH_4 variability in the troposphere and lower stratosphere, Atmos. Chem.Phys., 11, 12813–12837, https://doi.org/10.5194/acp-11-12813-2011

[18] Fung et al. (1991): Three-dimensional model synthesis of the global methane cycle, 20 July 1991. https://doi.org/10.1029/91JD01247

[19] Frankenberg et al. (2005): Assessing methane emissions from global space-borne observations, Science, 308, 1010–1014, doi:10.1126/science.1106644.

[20] Frankenberg et al. (2008): Tropical methane emissions: A revised view from SCIAMACHY onboard ENVISAT, Geophys. Res. Lett., 35, L15811, doi:10.1029/2008GL034300.

[21] Chandra et al. (2017): What controls the seasonal cycle of columnar methane observed by GOSAT over different regions in India?. Atmos. Chem. Phys., 17, 12633–12643, 2017, https://doi.org/10.5194/acp-17-12633-2017

[22] Sreenivas et al. (2019): Spatio- temporal distribution of CO_2 mixing ratio over Bhubaneswar, Varanasi and Jodhpur of India–Airborne campaign, 2016, Atmospheric Environment, https://doi.org/10.1016/j.atmosenv.2019.01.010

[23] Matthews et al. (1991): Methane emission from rice cultivation: Geographic and seasonal distribution of cultivated areas and emissions, Global Biogeochem. Cycles, 5(1), 3–24, doi:10.1029/90GB02311, 1991.

[24] Kaplan et al. (2006): Role of methane and biogenic volatile organic compound sources in late glacial and Holocene fluctuations of

atmospheric methane concentrations. Global Biogeochem. Cycles, 20(2), GB2016, doi:10.1029/2005GB002590

[25] Patra et al. (2009): Transport mechanisms for synoptic, seasonal and interannual SF_6 variations and "age" of air in troposphere, Atmos. Chem. Phys., 9(4), 1209–1225, doi:10.5194/acp-9-1209-2009

[26] Chen et al. (2010): High-accuracy continuous airborne measurements of greenhouse gases (CO_2 and CH_4) using the cavity ring-down spectroscopy (CRDS) technique, Atmos.Meas.Tech., 3, 375-386

Volume 8 MAY, 2019

Asia-Pacific GAW on Greenhouse Gases

Newsletter

Published by NIMS in May, 2019

Asia-Pacific GAW on Greenhouse Gases
Newsletter
National Institute of Meteorological Sciences
33, Seohobuk-ro, Seogwipo-si, Jeju-do, Republic of Korea
www.nims.go.kr